Chapter 10

The precise NLP model

Martin Schmidt, Marc C. Steinbach, Bernhard M. Willert

Abstract *In this chapter we describe a highly detailed nonlinear program (NLP) of gas networks for the case of fixed discrete decisions. By including nonlinear physics and a detailed description of the technical network devices, a level of accuracy is reached that is comparable to current commercial simulation software. Our NLP model is used to validate the solutions of the previously described models. A successful validation provides a solution of the underlying mixed-integer nonlinear program (MINLP).*

Short-term and mid-term planning problems in gas networks, such as the validation of nominations, involve gas dynamics in combination with complex technical devices. The laws of thermodynamics introduce partial differential equations (PDEs) and further nonlinear aspects to the problem. In addition, the switching between working modes of active (i.e., controllable) network elements is modeled by discrete decisions. A full consideration of all aspects leads to a *nonsmooth discrete-continuous control problem*, which after discretization of PDEs becomes a *nonsmooth mixed-integer nonlinear optimization problem* (nonsmooth MINLP).

The preceding Chapters 6 through 9 present four approaches that simplify the nonlinear aspects of the MINLP—amongst others by approximating the description of the gas flow—in order to determine suitable discrete decisions for the problem of validation of nominations. These previously discussed approaches are referred to as *decision approaches*, and any solution of a decision approach is considered a *solution candidate* for the original MINLP.

In contrast, this chapter presents a nonlinear optimization problem (NLP) based on a highly detailed model of stationary gas physics and technical devices. In this context we suppose that discrete decisions are already given, typically as result of one of the decision approaches, so that all discrete aspects can be removed from the MINLP. In fact, the main purpose of the NLP model is the *validation* of solution candidates obtained from the decision approaches: after fixing the discrete decisions, an initial iterate for the NLP model is generated from the continuous variables of the solution candidate (see Section 5.6). If the NLP solver converges to a (usually different) optimum, we have a feasible solution of the original MINLP that is locally optimal with respect to the fixed discrete decisions, and the given solution candidate has been confirmed to be a *valid* approximation to this

solution. If the validating NLP is *not* solved to optimality, no immediate conclusions can be drawn. For these cases, we introduce relaxed NLP models. Their impact is analyzed in detail in Section 10.3 and Chapter 11.

One important point remains to be mentioned: after discretizing the PDE constraints and fixing discrete decisions, we still have a nonsmooth optimization problem, but standard NLP theory, algorithms and solvers rely on smoothness (C^2), specifically to guarantee stability of solutions. Therefore we will apply reformulations and smoothing techniques to arrive at a standard NLP model,

$$\begin{aligned} \min_{x\in\mathbb{R}^n} \quad & f(x) \\ \text{s.t.} \quad & c_{\mathcal{E}}(x) = 0, \\ & c_{\mathcal{I}}(x) \geq 0, \\ & x \in [\underline{x}, \overline{x}], \end{aligned} \tag{10.1}$$

where $f\colon \mathbb{R}^n \to \mathbb{R}$ is the objective function and $c_{\mathcal{E}}\colon \mathbb{R}^n \to \mathbb{R}^m$, $c_{\mathcal{I}}\colon \mathbb{R}^n \to \mathbb{R}^k$ denote equality and inequality constraints, respectively, with $f, c_{\mathcal{E}}, c_{\mathcal{I}} \in C^2$.

The central part of this chapter is Section 10.1: here we formulate suitable component models for the relevant aspects of gas physics and for the individual element types of gas networks. We also discuss the discretization of PDE constraints and the direct approximation of their solutions, and we develop smoothing techniques where applicable. The component models are then combined to a standard NLP (10.1) in Section 10.4. Typical objective functions are presented in Section 10.2 and in Section 10.3 we consider relaxations of the NLP that we use to obtain further information in cases where no feasible solution is found.

10.1 ▪ Component models

The gas network is modeled as a directed graph $G = (V, A)$ with node set V and arc set A. The node set is partitioned into entries V_+, exits V_-, and inner nodes V_0. Gas is supplied to the network at entries and discharged at exits. At inner nodes, no gas is supplied or discharged.

The arc set is partitioned into pipes A_{pi}, resistors A_{rs}, short cuts A_{sc}, valves A_{va}, control valve stations A_{cv}, and compressor groups A_{cg}. Every arc $a = (u, v)$ connects a node u (called *tail*) to a different node v (called *head*). The notations $\delta^-(u)$ and $\delta^+(u)$ refer to the respective sets of incoming and outgoing arcs of u. The set of all incident arcs is $\delta(u) = \delta^-(u) \cup \delta^+(u)$.

Every network element has associated vectors of constraints and (continuous) variables. Throughout this chapter, constraints are denoted by c and vectors of variables by x, subscripted with indices or index sets; e.g., $c_{\mathcal{E}} = (c_i)_{i\in\mathcal{E}}$ is the vector of all equality constraints and $x_{A_{\text{pi}}} = (x_a)_{a\in A_{\text{pi}}}$ is the vector of all pipe variables.

Some gas quantities vary along arcs, so that their values at the head and tail may differ. If x is such a quantity, e.g., gas temperature, then the value on $a = (u, v)$ at u is written as $x_{a:u}$ and the value on a at v is denoted by $x_{a:v}$. These quantities are often mixed at nodes and thus are discontinuous across nodes, so that $x_{a:u} \neq x_{b:u}$ if $a \neq b \in \delta(u)$.

Finally, certain constraints depend on the *direction* of flow. To this end, we define flows from tail to head as positive and flows from head to tail as negative, and for every

node u we define respective sets of *inflow arcs* and *outflow arcs*:

$$\mathscr{I}(u) = \{a \in \delta^-(u) \mid q_a \geq 0\} \cup \{a \in \delta^+(u) \mid q_a \leq 0\},$$
$$\mathscr{O}(u) = \{a \in \delta^-(u) \mid q_a < 0\} \cup \{a \in \delta^+(u) \mid q_a > 0\}.$$

Now let x be a quantity that varies along arcs. The respective values of x at the *inflow node* and *outflow node* of $a = (u, v)$ are then written as

$$x_{a,\text{in}} = \begin{cases} x_{a:u}, & q_a \geq 0, \\ x_{a:v}, & q_a < 0, \end{cases} \qquad x_{a,\text{out}} = \begin{cases} x_{a:v}, & q_a \geq 0, \\ x_{a:u}, & q_a < 0. \end{cases} \tag{10.2}$$

Note that constraints that depend on $x_{a,\text{in}}$ or $x_{a,\text{out}}$ will typically be nonsmooth at $q_a = 0$.

We remark that most of the aspects discussed in this section are based on Chapter 2, where additional information can be found. Nevertheless, many formulas of Chapter 2 are restated here in order to fix the notation required to formulate the concrete NLP models.

10.1.1 ▪ Common model aspects

Here we present models of four basic physical phenomena that are relevant to several types of network elements. These phenomena depend on the gas composition, which is characterized by a *gas quality parameter vector* X with seven components (see Section 2.2): molar mass m, calorific value H_c, pseudocritical pressure p_c and temperature T_c, and coefficients of the molar isobaric heat capacity, $\tilde{A}, \tilde{B}, \tilde{C}$,

$$X = (m, H_c, p_c, T_c, \tilde{A}, \tilde{B}, \tilde{C}). \tag{10.3}$$

The first common aspect is the deviation of real (natural) gas from ideal gas, which is measured by the *compressibility factor* z; for ideal gas $z = 1$. Various empirical compressibility models have been developed; see Section 2.3.1. In our NLP model we use either the equation of the American Gas Association (AGA) (2.5), which is known to be sufficiently accurate for pressures up to 70 bar,

$$z^{\text{aga}}(p, T, p_c, T_c) = 1 + 0.257 p_r - 0.533 \frac{p_r}{T_r}, \quad \text{where} \quad p_r = \frac{p}{p_c}, \quad T_r = \frac{T}{T_c}, \tag{10.4}$$

or Papay's equation (2.4), which is appropriate for pressures up to 150 bar,

$$z^{\text{papay}}(p, T, p_c, T_c) = 1 - 3.52 p_r e^{-2.26 T_r} + 0.274 (p_r)^2 e^{-1.878 T_r}. \tag{10.5}$$

The constraint resulting from the chosen compressibility model is formulated as

$$0 = c^{\text{compr}}(z, p, T, p_c, T_c) = z - z^{\text{aga}}(p, T, p_c, T_c) \tag{10.6a}$$

or

$$0 = c^{\text{compr}}(z, p, T, p_c, T_c) = z - z^{\text{papay}}(p, T, p_c, T_c), \tag{10.6b}$$

where the concrete choice is up to the modeler. Several constraints described in the next sections make use of the partial derivatives

$$\frac{\partial z}{\partial p}(p, T, p_c, T_c) \quad \text{and} \quad \frac{\partial z}{\partial T}(p, T, p_c, T_c)$$

of the chosen compressibility model. We choose to substitute them directly into the constraints in which they appear, instead of representing them by auxiliary variables and additional constraints.

The second aspect is the *specific isobaric heat capacity* c_p, or equivalently the *molar isobaric heat capacity* $\tilde{c}_p = mc_p$; see Section 2.2. These quantities express the energy that is required to increase the temperature of one kilogram (or mol) of gas by one Kelvin at constant pressure. We use the molar heat capacity of real gas, which is expressed by the molar heat capacity of ideal gas $\tilde{c}_p^0$ and a correction term for real gas $\Delta\tilde{c}_p$:

$$\begin{aligned}
0 &= c^{\text{mhc-real}}(m, c_p, \tilde{c}_p^0, \Delta\tilde{c}_p) = mc_p - (\tilde{c}_p^0 + \Delta\tilde{c}_p),\\
0 &= c^{\text{mhc-ideal}}(\tilde{c}_p^0, T, \tilde{A}, \tilde{B}, \tilde{C}) = \tilde{c}_p^0 - (\tilde{A} + \tilde{B}T + \tilde{C}T^2),\\
0 &= c^{\text{mhc-corr}}(\Delta\tilde{c}_p, p, T, p_c, T_c)\\
&= \Delta\tilde{c}_p + R\int_0^p \frac{1}{\tilde{p}}\left(2T\frac{\partial z}{\partial T}(\tilde{p}, T, p_c, T_c) + T^2\frac{\partial^2 z}{\partial T^2}(\tilde{p}, T, p_c, T_c)\right)\mathrm{d}\tilde{p}.
\end{aligned}$$

Here, $\tilde{c}_p^0$ is modeled by a least-squares fit with parameters $\tilde{A}, \tilde{B}, \tilde{C}$. The partial derivatives of the compressibility factor are substituted in-place, hence $c^{\text{mhc-corr}}$ does not have z as an explicit argument. If the AGA formula (10.4) is chosen for the compressibility factor, the correction term for real gas vanishes, and the model of heat capacity reduces to the model for ideal gas. If Papay's equation is chosen instead, the analytical solution of the integral is used directly in $c^{\text{mhc-corr}}$, i.e.,

$$\begin{aligned}
&c^{\text{mhc-corr}}(\Delta\tilde{c}_p, p, T, p_c, T_c)\\
&\qquad = \Delta\tilde{c}_p + R\left(\left(\gamma\delta + \frac{1}{2}\gamma\delta^2 T_r\right)p_r^2 T_r e^{\delta T_r} - (2\alpha\beta + \alpha\beta^2 T_r)p_r T_r e^{\beta T_r}\right)
\end{aligned}$$

with constants

$$\alpha = 3.52, \quad \beta = -2.26, \quad \gamma = 0.274, \quad \delta = -1.878.$$

The full heat capacity model is given by the constraint vector

$$0 = c^{\text{heat-cap}}(p, T, X, x^{\text{heat-cap}}) = \begin{pmatrix} c^{\text{mhc-real}}(m, c_p, \tilde{c}_p^0, \Delta\tilde{c}_p)\\ c^{\text{mhc-ideal}}(\tilde{c}_p^0, T, \tilde{A}, \tilde{B}, \tilde{C})\\ c^{\text{mhc-corr}}(\Delta\tilde{c}_p, p, T, p_c, T_c)\end{pmatrix} \tag{10.7}$$

with associated variables

$$x^{\text{heat-cap}} = (c_p, \tilde{c}_p^0, \Delta\tilde{c}_p).$$

Another common aspect is the Joule–Thomson effect (see Section 2.2 for physical details), which describes the temperature change that results from any pressure change according to (2.6) and (2.7),

$$T_{\text{out}} - T_{\text{in}} = \int_{p_{\text{in}}}^{p_{\text{out}}} \mu_{\text{JT}}(p, T, m, c_p, p_c, T_c)\,\mathrm{d}p,$$

where

$$\mu_{\text{JT}}(p, T, m, c_p, p_c, T_c) = \frac{T}{p}\frac{R}{mc_p}\left(T\frac{\partial z}{\partial T}(p, T, p_c, T_c)\right).$$

Since the calculation of gas temperatures involves substantial inaccuracies, because exact environmental temperatures are usually not known for mid-term planning, a simple two-point finite difference approximation is usually sufficiently accurate, yielding the constraint

$$\begin{aligned} 0 &= c^{\mathrm{jt}}(p_{\mathrm{in}}, p_{\mathrm{out}}, T_{\mathrm{in}}, T_{\mathrm{out}}, X, \mu_{\mathrm{JT}}, c_{p,\mathrm{out}}) \\ &= \begin{pmatrix} \mu_{\mathrm{JT}} - \dfrac{T_{\mathrm{out}}}{p_{\mathrm{out}}} \dfrac{R}{m c_{p,\mathrm{out}}} \left(T_{\mathrm{out}} \dfrac{\partial z}{\partial T}(p_{\mathrm{out}}, T_{\mathrm{out}}, p_{\mathrm{c}}, T_{\mathrm{c}}) \right) \\ T_{\mathrm{out}} - T_{\mathrm{in}} - (p_{\mathrm{out}} - p_{\mathrm{in}}) \mu_{\mathrm{JT}} \end{pmatrix}. \end{aligned} \tag{10.8}$$

The last common phenomenon of gas physics is the interrelation of density ρ, pressure p, and temperature T. These gas quantities are coupled by the *thermodynamical standard equation of state for real gases* (2.20):

$$0 = c^{\mathrm{eos}}(p, T, \rho, m, z) = \rho z R T - p m. \tag{10.9}$$

10.1.2 ▪ Nodes

Every node $u \in V$ has a pressure variable p_u, a temperature variable T_u, and a vector of mixed gas parameters X_u (10.3). The incident arcs define relations between the pressures and temperatures of the connected nodes.

Nodes are assumed to have zero volume and hence satisfy a mass balance equation of Kirchhoff type:

$$0 = c_u^{\mathrm{flow}}(q_{\delta(u)}) = \sum_{a \in \delta^+(u)} q_a - \sum_{a \in \delta^-(u)} q_a - q_u^{\mathrm{nom}}. \tag{10.10}$$

Here, $q_{\delta(u)}$ contains the mass flows along the incident arcs, and q_u^{nom} denotes the externally supplied or discharged mass flow at u, which satisfies

$$\begin{aligned} q_u^{\mathrm{nom}} &\geq 0, \quad u \in V_+, \\ q_u^{\mathrm{nom}} &= 0, \quad u \in V_0, \\ q_u^{\mathrm{nom}} &\leq 0, \quad u \in V_-. \end{aligned}$$

These flows are typically fixed to values that are determined by the considered nomination. Thus, they are regarded as constants in this context. However, variables representing exchanged flows can easily be added to the model, if the supplied and discharged flows are not known a priori.

Gas flows entering node u are assumed to mix perfectly. The components of X mix according to the distribution of molar inflows $\hat{q} = q/m$, yielding a convex combination X_u for the outflow composition. The resulting constraint reads (see (2.9))

$$\begin{aligned} 0 &= c_u^{\mathrm{mix}}(q_{\delta(u)}, X_{\delta(u)}, X_u) \\ &= X_u \left(\hat{q}_u^{\mathrm{nom}} + \sum_{a \in \delta(u)} \hat{q}_a \right) - \left(\hat{q}_u^{\mathrm{nom}} X_u^{\mathrm{nom}} + \sum_{a \in \delta(u)} \hat{q}_a X_a \right). \end{aligned} \tag{10.11}$$

Here and in what follows, X_a is the vector of gas parameters of the gas in arc a and X_u represents the mixed gas of inflow arcs at node u. Both $\hat{q}_u^{\mathrm{nom}}$ and X_u^{nom} are given constants at entries $u \in V_+$ and are set to zero at other nodes $u \in V_- \cup V_0$. The mixed quality parameters are propagated to all outgoing arcs,

$$0 = c_{u,a}^{\mathrm{prop}}(X_u, X_a) = X_u - X_a \quad \text{for all } a \in \mathcal{O}(u).$$

The exact mixing equation for gas temperatures slightly differs from (10.11): it can be derived from the conservation of energy and involves the molar isobaric heat capacity $\tilde{c}_p$, yielding a convex combination with weights determined by the distribution of $\tilde{c}_p\hat{q} = c_p q$ (see (2.10)):

$$T_u = \frac{\tilde{c}^{\text{nom}}_{p,u}\hat{q}^{\text{nom}}_u T^{\text{nom}}_u + \sum_{a\in\mathscr{I}(u)} \tilde{c}_{p,a:u}\hat{q}_a T_{a:u}}{\tilde{c}^{\text{nom}}_{p,u}\hat{q}^{\text{nom}}_u + \sum_{a\in\mathscr{I}(u)} \tilde{c}_{p,a:u}\hat{q}_a}, \tag{10.12}$$

where T^{nom}_u is the (constant) temperature of the supplied gas at entries $u \in V_+$ and zero for all other nodes $u \in V_- \cup V_0$. Since (10.12) results in a quite complicated model, we approximate the equations of temperature mixing and propagation by assuming identical heat capacities, so that the corresponding factors in (10.12) cancel each other. The investigation of the quality of this approximation remains a topic of further research. The resulting constraints are:

$$\begin{aligned} 0 &= c^{\text{mix-temp}}_u(q_{\mathscr{I}(u)}, m_{\mathscr{I}(u)}, (T_{a:u})_{a\in\mathscr{I}(u)}, T_u) \\ &= T_u\Big(\hat{q}^{\text{nom}}_u + \sum_{a\in\mathscr{I}(u)} \hat{q}_a\Big) - \Big(\hat{q}^{\text{nom}}_u T^{\text{nom}}_u + \sum_{a\in\mathscr{I}(u)} \hat{q}_a T_{a:u}\Big), \end{aligned} \tag{10.13}$$

$$0 = c^{\text{prop-temp}}_{u,a}(T_u, T_{a:u}) = T_u - T_{a:u} \quad \text{for all } a \in \mathscr{O}(u). \tag{10.14}$$

Note that all mixing constraints are discontinuous since $\mathscr{I}(u)$ and $\mathscr{O}(u)$ depend on the flow directions. To obtain a smooth model, we fix all flow directions according to the candidate solution of the decision approach (by setting 0 as lower or upper bound on q_a). Letting x^{base}_a denote the common variables of all arc types (see the immediately following Section 10.1.3), the full set of constraints of node u becomes

$$0 = c_u(x_u, x^{\text{base}}_{\delta(u)}) = \begin{pmatrix} c^{\text{flow}}_u(q_{\delta(u)}) \\ c^{\text{mix}}_u(q_{\mathscr{I}(u)}, X_{\mathscr{I}(u)}, X_u) \\ (c^{\text{prop}}_{u,a}(X_u, X_a))_{a\in\mathscr{O}(u)} \\ c^{\text{mix-temp}}_u(q_{\mathscr{I}(u)}, m_{\mathscr{I}(u)}, (T_{a:u})_{a\in\mathscr{I}(u)}, T_u) \\ (c^{\text{prop-temp}}_{u,a}(T_u, T_{a:u}))_{a\in\mathscr{O}(u)} \end{pmatrix}$$

and the vector of variables at node u reads

$$x_u = (p_u, T_u, X_u).$$

10.1.3 ▪ Arcs

Every arc $a = (u, v) \in A$ has a mass flow variable q_a, variables for the gas temperatures at tail and head, $T_{a:u}$ and $T_{a:v}$, respectively, and a quality parameter vector X_a, yielding a common basic variable vector of all arc models:

$$x^{\text{base}}_a = (q_a, T_{a:u}, T_{a:v}, X_a).$$

The specific constraints of every arc type will be described separately below; in some cases they involve additional variables.

10.1.4 ▪ Pipes

Pipes outnumber all other elements of a gas network. They are the most essential elements and the only ones with a nonnegligible length, which transport the gas over large

distances. Due to friction at the inner wall and due to gravity (if the pipe is inclined), pressure and temperature change when gas flows through a pipe. In addition, there is heat exchange with the surrounding. As already explained in Section 2.3.1, this leads to highly complex gas dynamics described by a system of hyperbolic, partial differential equations (PDEs).

We consider a cylindrical pipe with diameter D, cross-sectional area $A = D^2\pi/4$, and slope $s \in [-1, +1]$ (the tangent of the inclination angle), so that the transient gas dynamics can be expressed by the one-dimensional PDE system of Euler equations (2.12)–(2.14) as derived in Feistauer (1993) and Lurie (2008):

$$\frac{\partial \rho}{\partial t} + \frac{1}{A}\frac{\partial q}{\partial x} = 0, \tag{10.15a}$$

$$\frac{1}{A}\frac{\partial q}{\partial t} + \frac{\partial p}{\partial x} + \frac{1}{A}\frac{\partial (q\,v)}{\partial x} + g\,\rho\,s + \lambda(q)\frac{|v|\,v}{2D}\rho = 0, \tag{10.15b}$$

$$\begin{aligned} A\rho\,c_p\Big(\frac{\partial T}{\partial t} + v\frac{\partial T}{\partial x}\Big) - A\Big(1 + \frac{T}{z}\frac{\partial z}{\partial T}\Big)\frac{\partial p}{\partial t} \\ - A\,v\frac{T}{z}\frac{\partial z}{\partial T}\frac{\partial p}{\partial x} + A\rho\,v\,g\,s + \pi D\,c_{\mathrm{HT}}(T - T_{\mathrm{soil}}) = 0, \end{aligned} \tag{10.15c}$$

Here x and t denote the spatial coordinate and time coordinate, respectively, and g, c_{HT}, and T_{soil} stand for the gravitational acceleration, the heat transfer coefficient, and the soil temperature, respectively. The friction factor $\lambda(q)$ in (10.15b) models frictional forces at the inner pipe walls; see Section 2.3.1. Given a specific pipe $a \in A_{\mathrm{pi}}$, the gas velocity v is related to the mass flow q, density ρ, and the cross-sectional pipe area A_a via (2.11) yielding the constraint

$$0 = c_a^{\text{vel-flow}}(q, v, \rho) = A_a\rho v - q. \tag{10.16}$$

Since we consider the stationary case, all partial derivatives with respect to time vanish, and with (10.16) the above PDE system reduces to a semi-implicit system of ordinary differential equations (ODEs) for q, p, and T; ρ and p are related by (10.9). Applying some minor transformations (e.g., multiplying with ρ and using the chain-rule) yields

$$\frac{\partial q}{\partial x} = 0, \tag{10.17a}$$

$$\rho\frac{\partial p}{\partial x} - \frac{q^2}{A^2}\frac{\partial \rho}{\partial x}\frac{1}{\rho} + g\rho^2 s + \lambda(q)\frac{|q|q}{2A^2D} = 0, \tag{10.17b}$$

$$q c_p\frac{\partial T}{\partial x} - \frac{qT}{\rho z}\frac{\partial z}{\partial T}\frac{\partial p}{\partial x} + q\,g\,s + \pi D c_{\mathrm{HT}}(T - T_{\mathrm{soil}}) = 0. \tag{10.17c}$$

The continuity equation (10.17a) readily implies that q is constant along the pipe, which justifies the use of a single mass flow variable q_a for every pipe a. The momentum equation (10.17b) models the pressure gradient in terms of impact pressure, gravitational forces and frictional forces, and the energy equation (10.17c) models the temperature gradient in terms of pressure changes, gravitational effects, and heat exchange with the surrounding soil. Figure 10.1 illustrates possible profiles of pressure and temperature along a pipe and the influence of the pipe diameter.

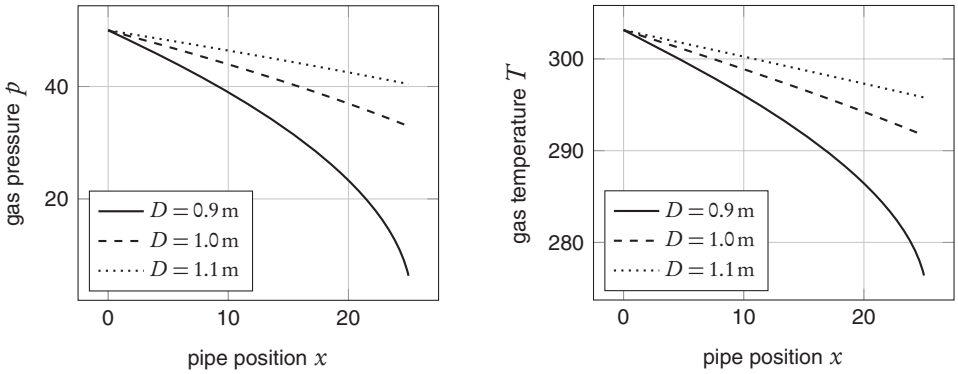

(a) Pressure profile; pressure in bar vs. pipe position in km.

(b) Temperature profile; temperature in K vs. pipe position in km.

Figure 10.1. *Pressure and temperature profiles of three horizontal pipes with different diameters ($L = 25$ km, $k = 0.06$ mm, $q = 500$ kg/s). (Source: Schmidt, Steinbach, and Willert (2014).)*

10.1.4.1 ▪ Smooth approximation of the friction term

Depending on which model of $\lambda(q)$ is chosen, the friction term $\lambda(q)|q|q$ in the momentum equation (10.17b) will be nonsmooth: the product $|q|q$ creates a second-order discontinuity at $q = 0$ if $\lambda(0) \neq 0$, and the piecewise reference model of $\lambda(q)$ defined by the formulas of Prandtl–Colebrook (2.17) and Hagen–Poiseuille (2.16) has a jump discontinuity at the transition between laminar and turbulent flow; see Chapter 2 for details.

To avoid discontinuities, we replace the entire friction term $\lambda(q)|q|q$ by a globally smooth approximation $\phi(q)$. This approximation has originally been developed for water networks by Burgschweiger, Gnädig, and Steinbach (2009) and Burgschweiger, Gnädig, and Steinbach (2009), and applies as well to gas networks (see Schmidt, Steinbach, and Willert (2014)). The corresponding constraint for a specific pipe $a \in A_{\mathrm{pi}}$ reads

$$0 = c_a^{\mathrm{friction}}(\phi_a, q_a) = \phi_a - \tilde{\lambda}_a \left(\sqrt{q_a^2 + e_a^2} + b_a + \frac{c_a}{\sqrt{q_a^2 + d_a^2}} \right) q_a. \tag{10.18}$$

As illustrated in Figure 10.2, our approximation (10.18) is asymptotically correct for $|q| \to \infty$ if the following parameters are used (see Burgschweiger, Gnädig, and Steinbach (2009)):

$$\tilde{\lambda}_a = (2\log_{10}\beta_a)^{-2}, \qquad b_a = 2\delta_a, \qquad c_a = (\ln\beta_a + 1)\delta_a^2 - \frac{e_a^2}{2},$$
$$\alpha_a = \frac{2.51 A_a \eta}{D_a}, \qquad \beta_a = \frac{k_a}{3.71 D_a}, \qquad \delta_a = \frac{2\alpha_a}{\beta_a \ln 10}.$$

Here, η and k_a denote the dynamic viscosity of gas and the roughness of the pipe (see Section 2.3.1). The two smoothing parameters $d_a, e_a > 0$ remain to be chosen by the modeler (see Schmidt, Steinbach, and Willert (2014); Burgschweiger, Gnädig, and Steinbach (2009)).

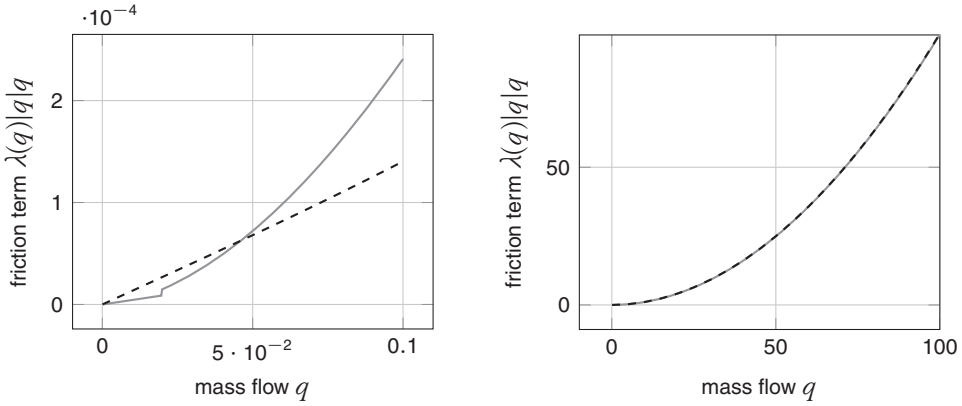

(a) Transition from laminar to turbulent flow. (b) Turbulent flow.

Figure 10.2. *Friction term $\lambda(q)|q|q$ according to Hagen–Poiseuille and Prandtl–Colebrook (——) and smooth approximation $\phi(q)$ with $d = e = 2.2$ (- - -) vs. mass flow q in* kg/s. *(Source: Schmidt, Steinbach, and Willert (2014).)*

10.1.4.2 ▪ ODE discretization

After obtaining a constant mass flow q_a from the continuity equation and smoothing the friction term, stationary gas dynamics are expressed by a spatial system of ODEs: a smooth version of the momentum equation (10.17b) and the unmodified smooth energy equation (10.17c). This system of two equations for the three variables (ρ, p, T) is completed by the equation of state (10.9); see the explanation for the general case in Section 2.3.1.

The standard procedure for converting ODE constraints to finite-dimensional NLP constraints is a discretization. Depending on the chosen grid, this results in a highly accurate model with a large number of nonlinear constraints. For simplicity, both in terms of implementation and presentation, we use an a priori discretization rather than an adaptive one: given a pipe $a \in A_{\mathrm{pi}}$, we choose some fixed grid, $0 = x_{a,0} < \cdots < x_{a,d} = L_a$. The continuous variables in (10.17b) and (10.17c) are then evaluated at the spatial grid points. To this end, we define the following abbreviations for $k = 0, \ldots, d$:

$$
\begin{aligned}
p_{a,k} &= p(x_{a,k}), & z_{a,k} &= z(p_{a,k}, T_{a,k}, p_{\mathrm{c},a}, T_{\mathrm{c},a}) && \text{(see (10.6))},\\
T_{a,k} &= T(x_{a,k}), & c_{p,a,k} &= c_p(p_{a,k}, T_{a,k}, X_a) && \text{(see (10.7))},\\
\rho_{a,k} &= \rho(x_{a,k}), & z_{T,a,k} &= \frac{\partial z}{\partial T}(p_{a,k}, T_{a,k}, p_{\mathrm{c},a}, T_{\mathrm{c},a}).
\end{aligned}
$$

Note that pressures $p_{a,0}$ and $p_{a,d}$ are identified with the pressure variables at the tail and head, p_u and p_v, respectively. In analogy, the temperature variables T_0 and T_d are identified with $T_{a:u}$ and $T_{a:v}$. Also for simplicity, we illustrate the ODE discretization with a two-point finite difference approach (backwards in space). Denoting step sizes by $\Delta x_{a,k} = x_{a,k} - x_{a,k-1}, k = 1, \ldots, d$, this yields the discrete pressure gradient

$$
p'(x_{a,k}) \approx \frac{p(x_{a,k}) - p(x_{a,k-1})}{\Delta x_{a,k}} =: \frac{\Delta p_{a,k}}{\Delta x_{a,k}}, \quad k = 1, \ldots, d,
$$

and similar gradient approximations for temperature and density. The discretized ODE constraints can then be written (for $k = 1, \dots, d$) as

$$\begin{aligned} 0 &= c_a^{\text{mom-discr}}(q_a, p_{a,k}, p_{a,k-1}, \rho_{a,k}, \rho_{a,k-1}, \phi_a) \\ &= \rho_{a,k} \frac{\Delta p_{a,k}}{\Delta x_{a,k}} - \frac{q_a^2}{A_a^2} \frac{\Delta \rho_{a,k}}{\Delta x_{a,k}} \frac{1}{\rho_{a,k}} + g \rho_{a,k}^2 s_a + \frac{\phi_a}{2 A_a^2 D_a}, \end{aligned} \tag{10.19a}$$

$$\begin{aligned} 0 &= c_a^{\text{ener-discr}}(q_a, p_{a,k}, p_{a,k-1}, T_{a,k}, T_{a,k-1}, \rho_{a,k}, z_{a,k}, c_{p,a,k}, p_{\text{c},a}, T_{\text{c},a}) \\ &= q_a c_{p,a,k} \frac{\Delta T_{a,k}}{\Delta x_{a,k}} - \frac{q_a T_{a,k}}{\rho_{a,k} z_{a,k}} z_{T,a,k} \frac{\Delta p_{a,k}}{\Delta x_{a,k}} + q_a g s_a \\ &\quad + \pi D_a c_{\text{HT,a}} (T_{a,k} - T_{\text{soil},a}). \end{aligned} \tag{10.19b}$$

The partial derivative $z_{T,a,k}$ is substituted directly in the constraint instead of introducing an additional variable and an according constraint. Next, we have to add the constraints for the equation of state, compressibility, and heat capacity in every grid point, obtaining (for $k = 1, \dots, d$)

$$\begin{aligned} 0 &= c_{a,k}^{\text{dyn}}(x_a^{\text{base}}, x_{a,k}^{\text{dyn}}, x_{a,k-1}^{\text{dyn}}, \phi_a, x_u, x_v) \\ &= \begin{pmatrix} c_a^{\text{mom-discr}}(q_a, p_{a,k}, p_{a,k-1}, \rho_{a,k}, \rho_{a,k-1}, \phi_a) \\ c_a^{\text{ener-discr}}(q_a, p_{a,k}, p_{a,k-1}, T_{a,k}, T_{a,k-1}, \rho_{a,k}, z_{a,k}, c_{p,a,k}, p_{\text{c},a}, T_{\text{c},a}) \\ c^{\text{eos}}(p_{a,k}, T_{a,k}, \rho_{a,k}, m_a, z_{a,k}) \\ c^{\text{compr}}(z_{a,k}, p_{a,k}, T_{a,k}, p_{\text{c},a}, T_{\text{c},a}) \\ c^{\text{heat-cap}}(p_{a,k}, T_{a,k}, X_a, x_{a,k}^{\text{heat-cap}}) \end{pmatrix}, \end{aligned} \tag{10.20}$$

where the required additional dynamic variables are defined as

$$\begin{aligned} x_{a,k}^{\text{dyn}} &= (p_{a,k}, T_{a,k}, \rho_{a,k}, z_{a,k}, x_{a,k}^{\text{heat-cap}}), && k = 1, \dots, d-1, \\ x_{a,k}^{\text{dyn}} &= (\rho_{a,k}, z_{a,k}, x_{a,k}^{\text{heat-cap}}), && k \in \{0, d\}. \end{aligned}$$

Together with the smooth approximation of the friction term, the complete model of the discretized dynamic system finally reads

$$\begin{aligned} 0 = c_a^{\text{dyn}}(x_a^{\text{base}}, x_a^{\text{dyn}}, x_u, x_v) &= \begin{pmatrix} c_a^{\text{friction}}(\phi_a, q_a) \\ \left(c_{a,k}^{\text{dyn}}(x_a^{\text{base}}, x_{a,k}^{\text{dyn}}, x_{a,k-1}^{\text{dyn}}, \phi_a, x_u, x_v)\right)_{k=1}^{d} \end{pmatrix}, \\ x_a^{\text{dyn}} &= (\phi_a, (x_{a,k}^{\text{dyn}})_{k=0}^{d}). \end{aligned}$$

Finally, we remark that one may also apply suitable higher order discretizations instead of the presented two-point finite differences scheme.

10.1.4.3 ▪ ODE approximation

A second possible approach for converting ODE constraints to finite-dimensional NLP constraints is the direct approximation of ODE solutions, which leads to fewer nonlinear equations with a reduced degree of accuracy as compared to a discretization.

In fact, the decision approaches of the preceding chapters drop the energy equation (10.17c) and use approximate solutions of the momentum equation (10.17b). This is an approach with a long tradition in gas engineering, so that suitable approximations are well

known and well tested. Specifically, by further neglecting the impact pressure term and assuming a mean compressibility factor $z_{\mathrm{m},a} = z(p_{\mathrm{m},a}, T_{\mathrm{m},a}, p_{\mathrm{c}}, T_{\mathrm{c}})$ (that can be assumed by using a mean pressure $p_{\mathrm{m},a}$ and a mean temperature $T_{\mathrm{m},a}$), solutions of the momentum equation (10.17b) can be approximated by the equation stated in Lemma 2.1,

$$\begin{aligned} 0 &= c_a^{\text{mom-approx}}(p_u, p_v, \phi_a, T_{\mathrm{m},a}, z_{\mathrm{m},a}, m_a) \\ &= p_v^2 - \left(p_u^2 - \Lambda_a \phi_a \frac{e^{S_a} - 1}{S_a} \right) e^{-S_a}, \end{aligned} \tag{10.21}$$

where the roughly quadratic dependence on q_a is hidden in the friction variable, $\phi_a \approx \lambda(q_a)|q_a|q_a$, and Λ_a, S_a are defined in terms of the above mean values:

$$\begin{aligned} \Lambda_a &= \Lambda_a(T_{\mathrm{m},a}, z_{\mathrm{m},a}, m_a) = \frac{L_a}{A_a^2 D_a} \frac{z_{\mathrm{m},a} T_{\mathrm{m},a} R}{m_a}, \\ S_a &= S_a(T_{\mathrm{m},a}, z_{\mathrm{m},a}, m_a) = 2 g L_a s_a \frac{m_a}{z_{\mathrm{m},a} T_{\mathrm{m},a} R}. \end{aligned}$$

More details on this approximation can be found in Chapter 2; suitable choices for the approximate mean values $p_{\mathrm{m},a}, T_{\mathrm{m},a}$ will be discussed below.

An approximation replaces the energy equation (10.17c) when an isothermal approach is not desired. It is derived by assuming a constant value for the specific heat capacity c_p and applying a two point finite difference. In addition, mean values for pressure $p_{\mathrm{m},a}$ and $T_{\mathrm{m},a}$ are used to obtain mean values for the compressibility factor $z_{\mathrm{m},a}$ and the density $\rho_{\mathrm{m},a}$, yielding (see Schmidt, Steinbach, and Willert (2014))

$$\begin{aligned} 0 &= c_a^{\text{ener-approx}}(q_a, p_{a,\mathrm{in}}, p_{a,\mathrm{out}}, T_{a,\mathrm{in}}, T_{a,\mathrm{out}}, \rho_{\mathrm{m},a}, p_{\mathrm{m},a}, T_{\mathrm{m},a}, z_{\mathrm{m},a}, p_{\mathrm{c},a}, T_{\mathrm{c},a}) \\ &= q_a \left(T_{a,\mathrm{out}} - T_{a,\mathrm{in}} + \frac{g s_a L_a}{c_p} \right) - \frac{z_{T,\mathrm{m},a}}{c_p \rho_{\mathrm{m},a} z_{\mathrm{m},a}} T_{a,\mathrm{out}} q_a (p_{a,\mathrm{out}} - p_{a,\mathrm{in}}) \\ &\quad + \frac{\pi D_a c_{\mathrm{HT,a}} L_a}{c_p} (T_{a,\mathrm{out}} - T_{\mathrm{soil},a}), \end{aligned} \tag{10.22}$$

where

$$z_{T,\mathrm{m},a} = \frac{\partial z}{\partial T}(p_{\mathrm{m},a}, T_{\mathrm{m},a}, p_{\mathrm{c},a}, T_{\mathrm{c},a})$$

is substituted directly. Recall the definition of direction-dependent variables: for positive flow we have

$$p_{a,\mathrm{in}} = p_u, \qquad p_{a,\mathrm{out}} = p_v, \qquad T_{a,\mathrm{in}} = T_{a:u}, \qquad T_{a,\mathrm{out}} = T_{a:v},$$

and in case of (strictly) negative flow the definitions read

$$p_{a,\mathrm{in}} = p_v, \qquad p_{a,\mathrm{out}} = p_u, \qquad T_{a,\mathrm{in}} = T_{a:v}, \qquad T_{a,\mathrm{out}} = T_{a:u}.$$

For $\rho_{\mathrm{m},a}$ we need an additional constraint for the equation of state (10.9). Alternatively, we can work with a further simplified model where $\rho_{\mathrm{m},a}$ is replaced by a constant mean value.

Figure 10.3 compares the temperature change according to the ODE (10.19b) and its approximation (10.22). On the left, the temperature profile along a pipe is illustrated and on the right the temperature profile for varying mass flow is presented.

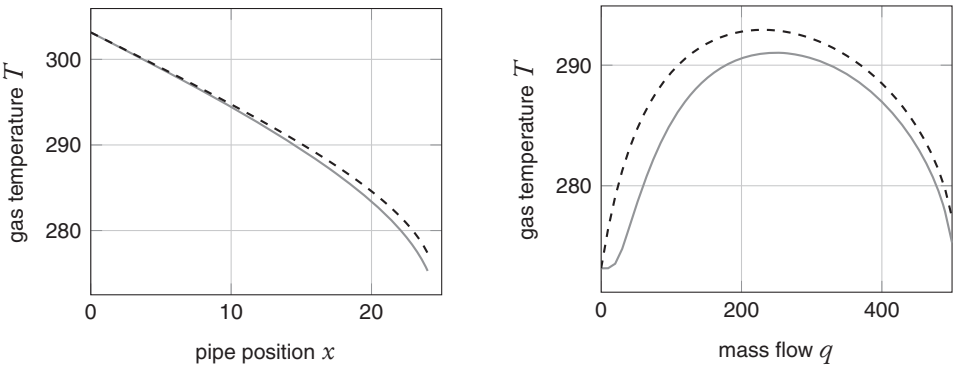

(a) Gas temperature in K vs. pipe position in km.

(b) Gas temperature in K vs. mass flow in kg/s.

Figure 10.3. *Gas temperature according to ODE discretization with* 40 *discretization steps (——) and approximation (- - -) ($L = 24$ km, $D = 1$ m, $k = 0.1$ mm, $q = 500$ kg/s). (Source: Schmidt, Steinbach, and Willert (2014).)*

The approximating constraints (10.21) and (10.22) make both use of approximate mean pressures $p_{\mathrm{m},a}$ and temperatures $T_{\mathrm{m},a}$. Several possibilities exist to define these values and to incorporate them into an NLP. A simple choice defines the values as constant averages of given variable bounds in

$$p_{\mathrm{m},a} = \frac{1}{2}\big(\max(\underline{p}_u, \underline{p}_v) + \min(\overline{p}_u, \overline{p}_v)\big), \tag{10.23a}$$

$$T_{\mathrm{m},a} = \frac{1}{2}\big(\max(\underline{T}_{a:u}, \underline{T}_{a:v}) + \min(\overline{T}_{a:u}, \overline{T}_{a:v})\big). \tag{10.23b}$$

In case of globally identical temperature bounds, (10.23b) can be simplified to

$$T_{\mathrm{m},a} = \frac{1}{2}(\underline{T} + \overline{T}).$$

A more sophisticated choice adds a constraint to include the mean values as variables that depend on pressures and temperatures at the pipe; see Menon (2005) and Eq. (2.28) in Section 2.3.1.2:

$$0 = c_a^{\mathrm{mean}}(p_{\mathrm{m},a}, T_{\mathrm{m},a}, p_u, p_v, T_{a:u}, T_{a:v}) = \begin{pmatrix} p_{\mathrm{m},a} - \frac{2}{3}\big(p_u + p_v - \frac{p_u p_v}{p_u + p_v}\big) \\ T_{\mathrm{m},a} - \frac{2}{3}(T_{a:u} + T_{a:v} - \frac{T_{a:u} T_{a:v}}{T_{a:u} + T_{a:v}}) \end{pmatrix}. \tag{10.24}$$

Since pressure and temperature profiles along a pipe have similar trends—see Figure 10.1—the same formula for the mean value is used. Alternatively, the arithmetic mean can be used for temperature. The full approximation model of a pipe is thus expressed by the constraints

$$\begin{aligned} 0 &= c_a^{\mathrm{dyn}}(x_a^{\mathrm{base}}, x_a^{\mathrm{dyn}}, x_u, x_v) \\ &= \begin{pmatrix} c_a^{\mathrm{friction}}(\phi_a, q_a) \\ c_a^{\mathrm{mom\text{-}approx}}(p_u, p_v, \phi_a, T_{\mathrm{m},a}, z_{\mathrm{m},a}, m_a) \\ c_a^{\mathrm{ener\text{-}approx}}(q_a, p_{a,\mathrm{in}}, p_{a,\mathrm{out}}, T_{a,\mathrm{in}}, T_{a,\mathrm{out}}, \rho_{\mathrm{m},a}, p_{\mathrm{m},a}, T_{\mathrm{m},a}, z_{\mathrm{m},a}, p_{\mathrm{c},a}, T_{\mathrm{c},a}) \\ c^{\mathrm{eos}}(p_{\mathrm{m},a}, T_{\mathrm{m},a}, \rho_{\mathrm{m},a}, m_a, z_{\mathrm{m},a}) \\ c^{\mathrm{compr}}(z_{\mathrm{m},a}, p_{\mathrm{m},a}, T_{\mathrm{m},a}, p_{\mathrm{c},a}, T_{\mathrm{c},a}) \\ c_a^{\mathrm{mean}}(p_{\mathrm{m},a}, T_{\mathrm{m},a}, p_u, p_v, T_{a:u}, T_{a:v}) \end{pmatrix} \end{aligned} \tag{10.25}$$

and variables

$$x_a^{\text{dyn}} = (\phi_a, p_{\text{m},a}, T_{\text{m},a}, z_{\text{m},a}, \rho_{\text{m},a}).$$

We remark that constraint (10.25) has the same name as constraint (10.20) since both can be used as alternatives in the complete NLP model. If (10.23) is chosen for the mean values, the model simplifies: the constraint c_a^{mean} is dropped, and $p_{\text{m},a}$ as well as $T_{\text{m},a}$ become constants.

10.1.4.4 ▪ Velocity constraint

The pressure change along a pipe induces changes of density and temperature, and also of gas velocity. Since high velocities can generate vibrations of the pipe (which in turn may lead to substantial noise emission or, worse, bursting of pipes), our model includes velocity limits for the gas flow. By (10.16), the velocity is related to density and mass flow, and (10.17) leads to a monotone change of pressure and temperature (with respect to the spatial coordinate). This results in a monotone change of density along the pipe due to the equation of state, and therefore the gas velocity is also monotone. It is thus sufficient to control the velocity at the end points of pipe $a = (u, v)$. The required additional variables, $x_a^{\text{vel}} = (v_{a:u}, v_{a:v}, \rho_{a:u}, \rho_{a:v}, z_{a:u}, z_{a:v})$, are determined by the constraints

$$0 = c_a^{\text{vel-1}}(x_a^{\text{base}}, x_a^{\text{vel}}, x_u, x_v) = \begin{pmatrix} c_a^{\text{vel-flow}}(q_a, v_{a:u}, \rho_{a:u}) \\ c_a^{\text{vel-flow}}(q_a, v_{a:v}, \rho_{a:v}) \\ c^{\text{eos}}(p_u, T_{a:u}, \rho_{a:u}, m_a, z_{a:u}) \\ c^{\text{eos}}(p_v, T_{a:v}, \rho_{a:v}, m_a, z_{a:v}) \\ c^{\text{compr}}(z_{a:u}, p_u, T_{a:u}, p_{\text{c},a}, T_{\text{c},a}) \\ c^{\text{compr}}(z_{a:v}, p_v, T_{a:v}, p_{\text{c},a}, T_{\text{c},a}) \end{pmatrix}. \tag{10.26}$$

If an ODE discretization scheme is used, the densities $\rho_{a:u}$ and $\rho_{a:v}$ coincide with the densities at the grid endpoints $\rho_{a,0}$ and $\rho_{a,d}$. This also holds for the compressibility factors, hence the two equations of state and the two constraints for the compressibility factors are already part of the model, and the velocity constraints reduce to

$$0 = c_a^{\text{vel-2}}(x_a^{\text{base}}, x_a^{\text{vel}}, x_a^{\text{dyn}}) = \begin{pmatrix} c_a^{\text{vel-flow}}(q_a, v_{a:u}, \rho_{a,0}) \\ c_a^{\text{vel-flow}}(q_a, v_{a:v}, \rho_{a,d}) \end{pmatrix}, \qquad x_a^{\text{vel}} = (v_{a:u}, v_{a:v}).$$

Any velocity limits are thus represented by bounds on the velocity variables x_a^{vel}.

10.1.4.5 ▪ Complete pipe model

Combining the constraints c_a^{dyn} and c_a^{vel}, we obtain the complete pipe model

$$0 = c_a(x_a, x_u, x_v) = \begin{pmatrix} c_a^{\text{dyn}}(x_a^{\text{base}}, x_a^{\text{dyn}}, x_u, x_v) \\ c_a^{\text{vel-1}}(x_a^{\text{base}}, x_a^{\text{vel}}, x_u, x_v) \end{pmatrix}$$

or

$$0 = c_a(x_a, x_u, x_v) = \begin{pmatrix} c_a^{\text{dyn}}(x_a^{\text{base}}, x_a^{\text{dyn}}, x_u, x_v) \\ c_a^{\text{vel-2}}(x_a^{\text{base}}, x_a^{\text{vel}}, x_a^{\text{dyn}}) \end{pmatrix},$$

with the variable vector $x_a = (x_a^{\text{base}}, x_a^{\text{dyn}}, x_a^{\text{vel}})$, depending on the required constraints for the gas velocity.

10.1.4.6 ▪ Comparison of model choices

As we have seen, several physical aspects allow for multiple modeling choices. The possible combinations lead to a broad variety of variants of the pipe constraints c_a, featuring different advantages and disadvantages.

A modestly accurate model combines the approximation (10.25) with the smooth friction model (10.18), the AGA compressibility model (10.4), and constant values of mean pressure and temperature (10.23), but assumes isothermal gas flow and thus drops the approximation of the energy equation from the model. Of all the presented alternative models for the relevant physical phenomena, this combination features the largest degree of similarity to the decision approaches described in Chapters 6–9, and a candidate solution generated by any decision approach will typically be a good initial point for NLP solution (see Section 5.6). The drawback is that this combination is in fact one of the most inaccurate choices of pipe models. Nevertheless, our experiences show that it proves to be reasonably accurate for several practical situations.

A very accurate pipe model combines a discretization of the Euler equations (10.20) with Papay's compressibility model (10.5). This leads to larger discrepancies with the models on which the decision approaches are based and tends to reduce the quality of candidate solutions as initial points for NLP solution. Moreover, it also tends to increase the likelihood that a feasible flow situation for the NLP will require different discrete decisions, and hence the probability that candidate solutions of the decision approaches will be rejected.

For a more detailed elaboration of these aspects we refer to Chapter 11.

10.1.5 ▪ Resistors

A resistor $a = (u, v) \in A_{\mathrm{rs}}$ is a fictitious network element that is used to account for pressure losses from components without an exact description in our model, such as measurement devices, narrow bends of pipes, filters, or internal station piping; see Section 2.3.2. The simpler of the two empirical models, which assumes a constant pressure loss $\xi_a > 0$ in the direction of flow, has a jump discontinuity in our context; see (2.32). The more elaborate resistor model of Darcy–Weisbach type formulates the pressure drop with a fictitious diameter D_a and a resistance coefficient $\zeta_a > 0$; see Section 2.3.2:

$$p_u - p_v = \frac{8\zeta_a}{\pi^2 D_a^4} \frac{q_a |q_a|}{\rho_{a,\mathrm{in}}}. \tag{10.27}$$

Here, (10.27) is obtained from (2.30) by replacing the velocity by the mass flow. Rather than a jump discontinuity, this model has only a second-order discontinuity at $q_a = 0$. Both nonsmooth aspects are handled by fixing the direction of flow according to the given candidate solution. In summary, the pressure loss of a resistor is given by the constraint

$$0 = \begin{cases} c_a^{\text{p-loss}}(q_a, p_u, p_v) = p_u - p_v - \operatorname{sgn}(q_a)\xi_a \ \text{ or} \\ c_a^{\text{p-loss}}(q_a, p_u, p_v, \rho_{a,\mathrm{in}}) = p_u - p_v - \dfrac{8\zeta_a}{\pi^2 D_a^4} \dfrac{q_a |q_a|}{\rho_{a,\mathrm{in}}}. \end{cases}$$

The inflow density $\rho_{a,\mathrm{in}}$ depends on the flow direction and correlates to the pressure, temperature, and compressibility factor either at the tail or at the head of the arc; see (10.2).

As always, the pressure loss induces a corresponding temperature decrease due to the Joule–Thomson effect (10.8). Thus, the full resistor model of a linear resistor reads

$$0 = c_a(x_u, x_v, x_a) = \begin{pmatrix} c_a^{\text{p-loss}}(q_a, p_u, p_v) \\ c_a^{\text{heat-cap}}(p_v, T_{a:v}, X_a, x_{a,\text{out}}^{\text{heat-cap}}) \\ c^{\text{jt}}(p_u, p_v, T_{a:u}, T_{a:v}, X_a, \mu_{\text{JT},a}, c_{p,a,\text{out}}) \end{pmatrix}, \tag{10.28}$$
$$x_a = (x_a^{\text{base}}, x_{a,\text{out}}^{\text{heat-cap}}, \mu_{\text{JT},a}).$$

The nonlinear model of a resistor is

$$0 = c_a(x_u, x_v, x_a) = \begin{pmatrix} c_a^{\text{p-loss}}(q_a, p_u, p_v, \rho_{a,\text{in}}) \\ c_a^{\text{heat-cap}}(p_v, T_{a:v}, X_a, x_{a,\text{out}}^{\text{heat-cap}}) \\ c^{\text{jt}}(p_u, p_v, T_{a:u}, T_{a:v}, X_a, \mu_{\text{JT},a}, c_{p,a,\text{out}}) \\ c^{\text{eos}}(p_{a,\text{in}}, T_{a,\text{in}}, \rho_{a,\text{in}}, m_a, z_{a,\text{in}}) \\ c^{\text{compr}}(z_{a,\text{in}}, p_{a,\text{in}}, T_{a,\text{in}}, p_{\text{c},a}, T_{\text{c},a}) \end{pmatrix}, \tag{10.29}$$
$$x_a = (x_a^{\text{base}}, x_{a,\text{out}}^{\text{heat-cap}}, \mu_{\text{JT},a}, \rho_{a,\text{in}}, z_{a,\text{in}}).$$

If the gas composition is uniform and the gas temperature is approximated by a mean value, i.e., no mixing equations are required, the pressure loss at resistors is the only model aspect left that depends on the flow direction. If a smooth approximation is applied, flow directions do not have to be fixed at any arc. See Section 9.1.3 for suitable nonlinear smoothings.

10.1.6 ▪ Valves

A valve $a = (u, v) \in A_{\text{va}}$ is an active element which can be *open* or *closed*. Valves are used to route the gas flow through the network, to decouple subnetworks, or to shut down sections of the network for maintenance. The discrete valve status is always fixed in our NLP context. An open valve has no impact on the flow (see Section 2.3.3) yielding identical inflow and outflow pressure and temperature,

$$0 = c_a(x_u, x_v, x_a) = \begin{pmatrix} p_u - p_v \\ T_{a,\text{in}} - T_{a,\text{out}} \end{pmatrix}, \quad x_a = x_a^{\text{base}}. \tag{10.30}$$

A closed valve simply acts like an absent arc: there is no flow through the valve, and the pressure and temperature of the connected nodes are completely decoupled,

$$0 = c_a(x_u, x_v, x_a) = q_a, \quad x_a = x_a^{\text{base}}. \tag{10.31}$$

10.1.7 ▪ Short cuts

Short cuts $a = (u, v) \in A_{\text{sc}}$ are again fictitious network elements introduced exclusively for modeling purposes, such as splitting a single physical exit with several customers into several virtual exits with just one customer each. A short cut does not impair the flow in any way, having the same model as an open valve; see (10.30).

10.1.8 ▪ Control valve stations with remote access

A control valve station with remote access $a = (u, v) \in A_{\text{cv}}$ is used to reduce the pressure in a controlled way. This is necessary in cases where customers or downstream networks

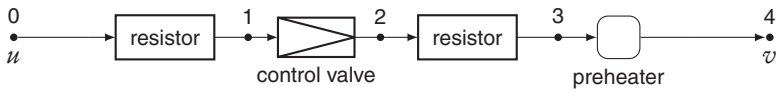

Figure 10.4. *Active control valve station (schematic overview). (Source: Schmidt, Steinbach, and Willert (2014).)*

require lower pressure levels than the usual pressure in transport pipelines. The remote access offers the operator a direct control of the pressure decrease. Note that control valve stations represent subnetworks that consist of several basic elements; see Section 2.3.4 and Section 2.4.1. The concrete layout depends on the considered network model. In our case, we use Figure 10.4 (but see also Figure 2.7, which models the bypass explicitly). In any case, control valve stations have a single inlet and a single outlet, so we consider entire stations as arcs in the NLP model.

Control valve stations possess three discrete operation modes: *active*, *bypass*, and *closed*. A *closed* control valve station acts like a closed valve. It blocks the gas flow and decouples the adjacent nodes; see (10.31). A control valve station in *bypass* mode lets the gas flow through the station in arbitrary direction and has no impact on pressure and temperature. It is modeled like an open valve (10.30).

The remainder of this section describes an *active* control valve station, which reduces the inflow pressure by a controllable amount, $\Delta_a \in [\underline{\Delta}_a, \overline{\Delta}_a]$. The pressure reduction works always in the positive direction of flow, i.e., from u to v; negative flow can only occur in bypass mode.

Additional devices like station piping or measurement devices generate further (uncontrolled) pressure losses that are accounted for with inlet and outlet resistors.

Because of the Joule–Thomson effect (10.8), the pressure reduction is always accompanied by a temperature decrease. Large pressure reductions may cause excessive temperature losses, which can lead to the undesirable process of gas hydrate formation. To prevent this, control valve stations contain a *gas preheater* that keeps the gas temperature above a given threshold value $\underline{T}_{a:v}$.

The control valve station is modeled as a subgraph; see Figure 10.4. When labeling the control valve itself as subarc $(1,2)$, the inlet resistor is subarc $(0,1)$, the outlet resistor is subarc $(2,3)$, and the preheater is subarc $(3,4)$. A complete active control valve station thus consists of four subarcs, where subnode 0 is identified with u and subnode 4 with v. Associated with every inner subnode are additional pressure, temperature, and heat capacity variables: $x_{a,i} = (p_{a,i}, T_{a,i}, x_{a,i}^{\text{heat-cap}})$, $i = 1,2,3$.

If the inlet resistor $(0,1) = (u,1)$ and outlet resistor $(2,3)$ are linear resistors, they are modeled based on (10.28),

$$\begin{aligned} 0 &= c_{a,(i,i+1)}(x_{a,i}, x_{a,i+1}, x_a^{\text{base}}, x_{a,(i,i+1)}) \\ &= \begin{pmatrix} c_{a,(i,i+1)}^{\text{p-loss}}(q_a, p_{a,i}, p_{a,i+1}) \\ c_{a,(i,i+1)}^{\text{heat-cap}}(p_{a,i+1}, T_{a,i+1}, X_a, x_{a,i+1}^{\text{heat-cap}}) \\ c_{a,(i,i+1)}^{\text{jt}}(p_{a,i}, p_{a,i+1}, T_{a,i}, T_{a,i+1}, X_a, \mu_{\text{JT},a,(i,i+1)}, c_{p,a,i+1}) \end{pmatrix}, \quad i = 0,2, \end{aligned} \tag{10.32}$$

with technical adjustments: The variable vector x_a of the model (10.28) is split into x_a^{base} and additional local variables $x_{a,(i,i+1)} = \mu_{\text{JT},a,(i,i+1)}$, $i = 0,2$, since the variables $x_{a,(i,i+1)}$ are specific for the inlet or outlet resistor, but mass flow and gas composition are associated with the station arc. In case of nonlinear resistors, the inlet and outlet resistors are modeled based on (10.29) with similar adjustments.

The control valve $(1,2)$ is modeled by a simple linear constraint,

$$0 = c^{\text{p-decr}}_{a,(1,2)}(p_{a,1}, p_{a,2}, \Delta_a) = p_{a,1} - p_{a,2} - \Delta_a.$$

Completed by the temperature decrease due to the Joule–Thomson effect, the control valve model reads

$$\begin{aligned} 0 &= c_{a,(1,2)}(x_{a,1}, x_{a,2}, x^{\text{base}}_a, x_{a,(1,2)}) \\ &= \begin{pmatrix} c^{\text{p-decr}}_{a,(1,2)}(p_{a,1}, p_{a,2}, \Delta_a) \\ c^{\text{heat-cap}}_{a,(1,2)}(p_{a,2}, T_{a,2}, X_a, x^{\text{heat-cap}}_{a,2}) \\ c^{\text{jt}}_{a,(1,2)}(p_{a,1}, p_{a,2}, T_{a,1}, T_{a,2}, X_a, \mu_{\text{JT},a,(1,2)}, c_{p,a,2}) \end{pmatrix}, \\ x_{a,(1,2)} &= (\Delta_a, \mu_{\text{JT},a,(1,2)}). \end{aligned}$$

The gas preheater is actually a feedback controller that measures the gas temperature at the station outlet to keep it above the threshold temperature $\underline{T}_{a:v}$ by preheating the gas at the station inlet, i.e., before pressure reduction. Since none of the decision approaches described in Chapters 6 through 9 consider a preheater, the activity status is not known a priori. Instead of modeling the feedback control, we obtain a simple model by considering a heating of the outlet gas,

$$T_{a:v} = \max(\underline{T}_{a:v}, T_{a,3}). \tag{10.33}$$

Since the maximum function is nonsmooth, we actually use the following smooth approximation of (10.33),

$$0 = c_{a,(3,4)}(p_{a,3}, p_v, T_{a,3}, T_{a:v}) = \begin{pmatrix} p_{a,3} - p_v \\ T_{a:v} - \underline{T}_{a:v} - \frac{1}{2}\left(\sqrt{\Delta T_a^2 + \varepsilon} + \Delta T_a\right) \end{pmatrix},$$

where $\Delta T_a = T_{a,3} - \underline{T}_{a:v}$ and $\varepsilon > 0$ is a suitable smoothing parameter. If the resistors of the station are linear, this model is logically equivalent to a feedback control model, since the temperature does not influence any other quantity. However, the pressure loss at nonlinear resistors depends on the inflow density at the resistor, which in turn depends on the inflow temperature. A higher inflow temperature results in a smaller density and thus a larger pressure loss at the resistor. The larger pressure loss at the resistor in a feedback control model is compensated by the control valve in the simple model, as long as the maximum pressure reduction of the control valve is not reached.

The complete model of an active control valve station with remote access then reads

$$\begin{aligned} 0 = c_a(x_u, x_v, x_a) &= \begin{pmatrix} c_{a,(0,1)}(x_u, x_{a,1}, x^{\text{base}}_a, x_{a,(0,1)}) \\ c_{a,(1,2)}(x_{a,1}, x_{a,2}, x^{\text{base}}_a, x_{a,(1,2)}) \\ c_{a,(2,3)}(x_{a,2}, x_{a,3}, x^{\text{base}}_a, x_{a,(2,3)}) \\ c_{a,(3,4)}(x_{a,3}, x_v, x^{\text{base}}_a) \end{pmatrix}, \\ x_a &= (x^{\text{base}}_a, x_{a,1}, x_{a,2}, x_{a,3}, x_{a,(0,1)}, x_{a,(1,2)}, x_{a,(2,3)}). \end{aligned} \tag{10.34}$$

10.1.9 ▪ Control valve stations without remote access

Some control valve stations lack the remote access featured by the previously described control valves. Instead of controlling the pressure loss directly, a threshold pressure value p^{set} is preset in this case. Since changing this preset pressure requires manual adjustments on-site, it is handled as a constant parameter in our model.

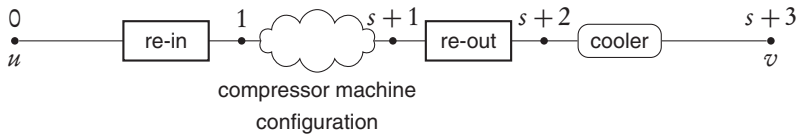

Figure 10.5. *Active compressor group (schematic overview). (Source: Schmidt, Steinbach, and Willert (2014).)*

The state of a control valve station without remote access $a = (u, v)$ depends on the pressures inside the station in relation to the preset pressure. The control valve station is active if the inflow pressure of the control valve lies above the preset pressure. If the pressure level in the downstream network requires a higher pressure at the head v than the threshold value, the control valve closes automatically. If the control valve does not need to reduce the pressure, i.e., the pressure at the head is smaller than the preset pressure threshold and the inflow and outflow pressures of the control valve are equal, the control valve is in bypass mode.

The model of a control valve station without remote access uses the same station graph as in Section 10.1.8. Note that, in contrast to control valves with remote access, the station resistors and the gas preheater are not circumvented in bypass, but cause a pressure reduction and temperature change.

Based on the given discrete decisions, a closed control valve is modeled by setting

$$\underline{p}_v = p_{a,1}, \quad q_a = 0.$$

In case of an active control valve station, the pressure loss at the control valve $\Delta_a = p_1 - p_2$ and the flow q_a must be nonnegative. Furthermore, the pressure at the head p_u is fixed to p_a^{set}. The pressure reduction results in a temperature change due to the Joule–Thomson effect.

The bypass mode is modeled by setting

$$\Delta_a = 0, \quad \overline{p}_v = p_a^{\text{set}}.$$

The resistors and the gas preheater are modeled as described in Section 10.1.8.

10.1.10 ▪ Compressor groups

While control valve stations reduce the gas pressure, compressor groups $a = (u, v) \in A_{\text{cg}}$ increase the gas pressure to compensate for the pressure loss caused by friction. Like control valve stations, compressor groups represent subnetworks with a single inlet and a single outlet. They also operate in the three discrete modes *active*, *bypass*, and *closed*, where the closed mode is again modeled like a closed valve, (10.31), and the bypass mode is again modeled like an open valve, (10.30). Here, the operation mode is always fixed according to a solution candidate from a decision approach.

In the remainder of this section, we concentrate on the active mode, where the direction of flow must be nonnegative, $q_a \geq 0$. The compressor group is modeled as a subgraph consisting of the following elements: several compressor machines that can be operated in a number of arrangements called *configurations*, an inlet resistor and an outlet resistor, and a *gas cooler* that reduces the outlet gas temperature if necessary. A compressor configuration is a serial connection of s subgroups (*stages*) of parallel compressor machines, to be described in more detail below. As illustrated in Figure 10.5, these elements are modeled as subarcs $(i, i+1)$, $i = 0, \ldots, s+2$, where subnode 0 is identified with u and subnode

$s+3$ with v. Associated with every inner subnode is a variable vector, $x_{a,i} = (p_{a,i}, T_{a,i})$, $i = 1,\dots,s+2$.

The models of all other elements described so far represent all physical or technical bounds by variable bounds, e.g., limits of the gas velocity are represented by bounds of the velocity variable at pipes. In contrast, the model of an active compressor group consists of equality constraints $c_{\mathscr{E},a}$ and nontrivial inequality constraints $c_{\mathscr{I},a}$. The inequality constraints will be needed to describe operating ranges of individual compressor machines. (The closed mode and bypass mode do not require inequality constraints.)

In the following we describe the subelements of an active compressor group. Subarc $(0,1)$ represents the inlet resistor,

$$0 = c_{a,(0,1)}(x_{a,0}, x_{a,1}, x_a^{\text{base}}, x_{a,(0,1)}),$$
$$x_{a,(0,1)} = (x_{a,1}^{\text{heat-cap}}, \mu_{\text{JT},a,(0,1)}),$$

and subarc $(s+1, s+2)$ represents the outlet resistor

$$0 = c_{a,(s+1,s+2)}(x_{a,s+1}, x_{a,s+2}, x_a^{\text{base}}, x_{a,(s+1,s+2)}),$$
$$x_{a,(s+1,s+2)} = (x_{a,s+2}^{\text{heat-cap}}, \mu_{\text{JT},a,(s+1,s+2)}).$$

Both resistors are modeled identically to the resistors in a control valve station; see (10.32). The gas cooler represented by the final subarc $(s+2, s+3)$ is modeled like the gas preheater in a control valve station, except that it keeps the outlet gas temperature below the threshold value $\overline{T}_{a:v}$ rather than above it:

$$T_{a:v} = \min(T_{a,s+2}, \overline{T}_{a:v}).$$

Again we approximate the nonsmooth equation with a smooth constraint,

$$0 = c_{a,(s+2,s+3)}(p_{a,s+2}, p_v, T_{a,s+2}, T_{a:v}) = \begin{pmatrix} p_{a,s+2} - p_v \\ T_{a:v} - \overline{T}_{a:v} + \frac{1}{2}\left(\sqrt{\Delta T_a^2 + \varepsilon} - \Delta T_a\right) \end{pmatrix},$$

where $\Delta T_a = T_{a,s+2} - \overline{T}_{a:v}$, and $\varepsilon > 0$ is a suitable smoothing parameter.

10.1.10.1 ▪ Configurations

The configurations of a compressor group form a discrete set of possible choices. The particular choice to be considered in the NLP model is determined by the candidate solution of a decision approach. Let us denote the subarcs associated with the given configuration by $(l, l+1)$, $l = 1,\dots,s_a$, where s_a is the number of serial stages of the configuration. Each stage l may contain m_l compressor machines. For example, the schematic compressor station in Figure 5.1(c) consists of two stages ($s_a = 2$) and two compressor machines each ($m_1 = m_2 = 2$). Finally, individual compressor machines at stage l of compressor group a will be referred to by $a(l,k)$, $k = 1,\dots,m_l$, and the mass flow through machine $a(l,k)$ will be denoted as $q_{a(l,k)}$. The total mass flow through the compressor group is distributed over the parallel machines at every stage,

$$0 = c_{a,l}^{\text{flow-dist}}(q_a, (q_{a(l,k)})_{k=1}^{m_l}) = q_a - \sum_{k=1}^{m_l} q_{a(l,k)}, \qquad l = 1,\dots,s_a.$$

Thus, the flows through the individual parallel machines do not have to be equal. In general, the inlet values of p and T at the parallel machines at stage $l+1$ are identical

and determined by the outlet values of stage l. The outlet pressures of parallel machines are also identical; we denote their common value by $p_{a,l+1}$. In contrast, the outlet temperatures $T^{\text{out}}_{a(l,k)}$ are usually different, since individual compressor machines may work at different operating points. The outlet temperatures then mix according to (10.13). Since all gas streams have identical composition, the molar masses cancel each other and (10.13) simplifies to

$$\begin{aligned} 0 &= c^{\text{mix-temp}}((q_{a(l,k)})_{k=1}^{m_l}, T_{a,l+1}, (T^{\text{out}}_{a(l,k)})_{k=1}^{m_l}) \\ &= T_{a,l+1} \sum_{k=1}^{m_l} q_{a(l,k)} - \sum_{k=1}^{m_l} q_{a(l,k)} T^{\text{out}}_{a(l,k)} \end{aligned}$$

for all stages $l = 1, \ldots, s_a$.

10.1.10.2 ▪ Compressor machines

The actual pressure increase at a compressor group is realized by compressor machines. Essentially two kinds of machines are commonly used: turbo compressors and piston compressors. These two types are based on different mechanical principles, leading to different physical and technical properties and to different applications (see Section 2.3.5.1 for details). We first describe basic features and principles that both compressor types have in common.

The energy that is required to compress a certain mass of gas is expressed by the specific change in adiabatic enthalpy H_{ad}, which depends primarily on the compression ratio $p_{\text{out}}/p_{\text{in}}$. For machine $a(l,k)$, it is modeled by the constraint

$$\begin{aligned} 0 &= c^{\text{ad-ent}}(H_{\text{ad},a(l,k)}, p_{a,l}, T_{a,l}, p_{a,l+1}, z_{a,l}, m_a, \varkappa_{a(l,k)}) \\ &= H_{\text{ad},a(l,k)} - \frac{z_{a,l} T_{a,l} R}{m_a r_{a(l,k)}} \left(\left(\frac{p_{a,l+1}}{p_{a,l}} \right)^{r_{a(l,k)}} - 1 \right), \quad r_{a(l,k)} = \frac{\varkappa_{a(l,k)} - 1}{\varkappa_{a(l,k)}}. \end{aligned} \tag{10.35}$$

The compression is assumed to be *isentropic*, more precisely it is adiabatic and reversible, and $\varkappa_{a(l,k)}$ denotes the *isentropic exponent* (see following subsection).

The power P that is required to increase the pressure depends on the mass flow q through the machine, the specific change in adiabatic enthalpy H_{ad}, and the adiabatic efficiency η_{ad}:

$$0 = c^{\text{power}}(P_{a(l,k)}, q_{a(l,k)}, H_{\text{ad},a(l,k)}, \eta_{\text{ad},a(l,k)}) = P_{a(l,k)} - \frac{q_{a(l,k)} H_{\text{ad},a(l,k)}}{\eta_{\text{ad},a(l,k)}}. \tag{10.36}$$

Isentropic exponent The value $\varkappa_{a(l,k)}$ used above depends on the gas state during the entire compression process. Several approximate models of this *isentropic exponent* exist. In our most detailed model choice, $\varkappa_{a(l,k)}$ is an arithmetic mean value,

$$c^{\text{isen-exp-mean}}(\varkappa_{a(l,k)}, \varkappa^{\text{in}}_{a(l,k)}, \varkappa^{\text{out}}_{a(l,k)}) = \varkappa_{a(l,k)} - \frac{1}{2}(\varkappa^{\text{in}}_{a(l,k)} + \varkappa^{\text{out}}_{a(l,k)}),$$

where $\varkappa^{\text{in}}_{a(l,k)}$ and $\varkappa^{\text{out}}_{a(l,k)}$ are the respective isentropic exponents at the compressor inlet and outlet, respectively. The latter are defined by (see Doering, Schedwill, and Dehli (2012)):

$$\begin{aligned} 0 &= c^{\text{isen-exp-def}}(\varkappa, p, T, z, c_p, m, p_{\text{c}}, T_{\text{c}}) \\ &= \varkappa - \frac{m c_p z}{m c_p Z_p(z, p, T, p_{\text{c}}, T_{\text{c}}) - R Z_T(z, p, T, p_{\text{c}}, T_{\text{c}})^2}, \end{aligned} \tag{10.37}$$

where we use the abbreviations

$$Z_p(z,p,T,p_c,T_c) = z - p\frac{\partial z}{\partial p}(p,T,p_c,T_c),$$
$$Z_T(z,p,T,p_c,T_c) = z + T\frac{\partial z}{\partial T}(p,T,p_c,T_c).$$

The complete model of the isentropic exponent thus becomes

$$\begin{aligned} 0 &= c^{\text{isen-exp}}(p_{a,l}, T_{a,l}, z_{a,l}, p_{a,l+1}, T^{\text{out}}_{a(l,k)}, z^{\text{out}}_{a(l,k)}, x^{\text{base}}_a, x^{\text{isen-exp}}_{a(l,k)}) \\ &= \begin{pmatrix} c^{\text{isen-exp-mean}}(\varkappa_{a(l,k)}, x^{\text{in}}_{a(l,k)}, x^{\text{out}}_{a(l,k)}) \\ c^{\text{isen-exp-def}}(x^{\text{in}}_{a(l,k)}, p_{a,l}, T_{a,l}, z_{a,l}, c_{p,a(l,k),\text{in}}, m_a, p_{c,a}, T_{c,a}) \\ c^{\text{heat-cap}}(p_{a,l}, T_{a,l}, X_a, x^{\text{heat-cap}}_{a(l,k),\text{in}}) \\ c^{\text{isen-exp-def}}(x^{\text{out}}_{a(l,k)}, p_{a,l+1}, T^{\text{out}}_{a(l,k)}, z^{\text{out}}_{a(l,k)}, c_{p,a(l,k),\text{out}}, m_a, p_{c,a}, T_{c,a}) \\ c^{\text{heat-cap}}(p_{a,l+1}, T^{\text{out}}_{a(l,k)}, X_a, x^{\text{heat-cap}}_{a(l,k),\text{out}}) \end{pmatrix} \end{aligned} \tag{10.38}$$

with additional variables

$$x^{\text{isen-exp}}_{a(l,k)} = (\varkappa_{a(l,k)}, x^{\text{in}}_{a(l,k)}, x^{\text{out}}_{a(l,k)}, x^{\text{heat-cap}}_{a(l,k),\text{in}}, x^{\text{heat-cap}}_{a(l,k),\text{out}}).$$

Here, $z_{a,l}$ and $z^{\text{out}}_{a(l,k)}$ represent the respective compressibility factors at the compressor inlet and outlet, which we need to compute $x^{\text{in}}_{a(l,k)}$ and $x^{\text{out}}_{a(l,k)}$. The values $c_{p,a(l,k),\text{in}}$ and $c_{p,a(l,k),\text{out}}$ are the corresponding specific isobaric heat capacities; these are part of the vectors $x^{\text{heat-cap}}_{a(l,k),\text{in}}$ and $x^{\text{heat-cap}}_{a(l,k),\text{out}}$, respectively.

A suitable simplified model for $\varkappa$ is obtained if we replace (10.37) by a linear function of the temperature (see LIWACOM (2004)),

$$\begin{aligned} 0 &= c^{\text{isen-exp}}(T_{a,l}, T^{\text{out}}_{a(l,k)}, x^{\text{isen-exp}}_{a(l,k)}) \\ &= \begin{pmatrix} \varkappa_{a(l,k)} - 1.296 + 5.8824 \times 10^{-4}(T_{\text{m},a(l,k)} - T_0) \\ T_{\text{m},a(l,k)} - \frac{1}{2}(T_{a,l} + T^{\text{out}}_{a(l,k)}) \end{pmatrix}, \\ x^{\text{isen-exp}}_{a(l,k)} &= (\varkappa_{a(l,k)}, T_{\text{m},a(l,k)}). \end{aligned} \tag{10.39}$$

The coarsest model choice for $\varkappa$ is a constant value, such as $\varkappa_{a(l,k)} = 1.296$, which is obtained from (10.39) with $T_{\text{m},a(l,k)} = T_0$. This model is either formulated by the constraint

$$0 = c^{\text{isen-exp}}(\varkappa_{a(l,k)}) = \varkappa_{a(l,k)} - 1.296, \tag{10.40}$$

or by replacing the variable $\varkappa$ with the constant value in all other constraints.

Temperature increase Due to the Joule–Thomson effect, the pressure increase at a compressor machine $a(l,k)$ causes a corresponding temperature increase for which several empirical models exist (see LIWACOM (2004)): the *isentropic equation model*, the *standard model*, and the *RG*1991 *model*. All these models can be interpreted as special cases of a fixed-point iteration that is initialized with the temperature increase of an ideal gas (see Schmidt, Steinbach, and Willert (2014)):

$$T^{\text{out},i+1}_{a(l,k)} = T^{\text{out,ideal}}_{a(l,k)} \frac{z(p_{a,l}, T_{a,l})}{z(p_{a,l+1}, T^{\text{out},i}_{a(l,k)})}, \quad T^{\text{out},0}_{a(l,k)} = T^{\text{out,ideal}}_{a(l,k)}, \quad i = 0,1,2,\dots .$$

The models mentioned above differ in the number of iterations and in the choice of the initial iterate $T^{\text{out,ideal}}_{a(l,k)}$. Here we consider only the standard model which uses a single fixed-point iteration, i.e., $T^{\text{out}}_{a(l,k)} = T^{\text{out},1}_{a(l,k)}$, and defines

$$T^{\text{out,ideal}}_{a(l,k)} = T_{a,l}\left(\frac{p_{a,l+1}}{p_{a,l}}\right)^{(\varkappa_{a(l,k)}-1)/(\varkappa_{a(l,k)}\eta_{\text{ad},a(l,k)})}.$$

This results in the constraints

$$\begin{aligned} 0 &= c^{\text{temp-inc}}(T^{\text{out,ideal}}_{a(l,k)}, T_{a,l}, p_{a,l}, p_{a,l+1}, \varkappa_{a(l,k)}, \eta_{\text{ad},a(l,k)}, \\ &\qquad z^{\text{out,temp-ideal}}_{a(l,k)}, p_{\text{c},a}, T_{\text{c},a}, T^{\text{out}}_{a(l,k)}, z_{a,l}) \\ &= \begin{pmatrix} T^{\text{out,ideal}}_{a(l,k)} - T_{a,l}\left(\frac{p_{a,l+1}}{p_{a,l}}\right)^{(\varkappa_{a(l,k)}-1)/(\varkappa_{a(l,k)}\eta_{\text{ad},a(l,k)})} \\ c^{\text{compr}}(z^{\text{out,temp-ideal}}_{a(l,k)}, p_{a,l+1}, T^{\text{out,ideal}}_{a(l,k)}, p_{\text{c},a}, T_{\text{c},a}) \\ T^{\text{out}}_{a(l,k)} - T^{\text{out,ideal}}_{a(l,k)} z_{a,l}/z^{\text{out,temp-ideal}}_{a(l,k)} \end{pmatrix}. \end{aligned} \tag{10.41}$$

Common machine model We are now ready to state the common part of the models for turbo compressors and piston compressors. Both types of compressor machines involve the volumetric flow in their specific descriptions, $Q = q/\rho$. In addition to the constraints described so far, we thus need a further constraint c^{eos} to determine the gas density at the machine inlet. Together with (10.35), (10.36), (10.38) or (10.39), and (10.41) this results in the constraint

$$\begin{aligned} 0 &= c^{\text{base}}_{a(l,k)}(x^{\text{base}}_a, x_{a,l}, x_{a,l+1}, x^{\text{base}}_{a(l,k)}, T^{\text{out,ideal}}_{a(l,k)}, z^{\text{out,temp-ideal}}_{a(l,k)}) \\ &= \begin{pmatrix} c^{\text{ad-ent}}(H_{\text{ad},a(l,k)}, p_{a,l}, T_{a,l}, p_{a,l+1}, z_{a,l}, m_a, \varkappa_{a(l,k)}) \\ c^{\text{power}}(P_{a(l,k)}, q_{a(l,k)}, H_{\text{ad},a(l,k)}, \eta_{\text{ad},a(l,k)}) \\ c^{\text{isen-exp}}(p_{a,l}, T_{a,l}, z_{a,l}, p_{a,l+1}, T^{\text{out}}_{a(l,k)}, z^{\text{out}}_{a(l,k)}, x^{\text{base}}_a, x^{\text{isen-exp}}_{a(l,k)}) \\ c^{\text{temp-inc}}(T^{\text{out,ideal}}_{a(l,k)}, T_{a,l}, p_{a,l}, p_{a,l+1}, \varkappa_{a(l,k)}, \eta_{\text{ad},a(l,k)}, \\ \qquad z^{\text{out,temp-ideal}}_{a(l,k)}, p_{\text{c},a}, T_{\text{c},a}, T^{\text{out}}_{a(l,k)}, z_{a,l}) \\ c^{\text{compr}}(z_{a,l}, p_{a,l}, T_{a,l}, p_{\text{c},a}, T_{\text{c},a}) \\ c^{\text{eos}}(p_{a,l}, T_{a,l}, \rho^{\text{in}}_{a(l,k)}, m_a, z_{a,l}) \end{pmatrix} \end{aligned} \tag{10.42}$$

with variables

$$x^{\text{base}}_{a(l,k)} = (q_{a(l,k)}, P_{a(l,k)}, H_{\text{ad},a(l,k)}, \eta_{\text{ad},a(l,k)}, T^{\text{out}}_{a(l,k)}, z_{a,l}, z^{\text{out}}_{a(l,k)}, \rho^{\text{in}}_{a(l,k)}, x^{\text{isen-exp}}_{a(l,k)}).$$

The complete set of constraints of every compressor machine then consists of (10.42) and type-specific technical restrictions. Many of these additional restrictions are modeled by least-squares fits based on measurements. For the resulting quadratic and biquadratic polynomials we use the notation introduced in Chapter 2; see (2.45) and (2.46). The specific model components of turbo compressors and piston compressors will now be discussed in detail.

Turbo compressor Turbo compressors are designed for large throughput at moderate compression ratios. From a mathematical point of view they are the most complex

network elements besides pipes. More details on turbo compressors are given in Section 2.3.5.1.

Every turbo compressor has an *operating range* representing the feasible *working points*. A working point is a pair of volumetric flow rate and specific change in adiabatic enthalpy. The operating range is described by a *characteristic diagram* as in Figure 2.4(a). This characteristic diagram is defined by the isolines of speed (2.47) and isolines of adiabatic efficiency (2.48). In our NLP model, the isolines of compressor $a(l,k)$ are given by the respective constraints

$$\begin{aligned}
0 &= c^{\text{speed}}_{a(l,k)}(H_{\text{ad},a(l,k)}, q_{a(l,k)}, \rho^{\text{in}}_{a(l,k)}, n_{a(l,k)}) \\
&= H_{\text{ad},a(l,k)} - \chi\left(\frac{q_{a(l,k)}}{\rho^{\text{in}}_{a(l,k)}}, n_{a(l,k)}; A^{\text{speed}}_{a(l,k)}\right), \\
0 &= c^{\text{eff}}_{a(l,k)}(\eta_{\text{ad},a(l,k)}, q_{a(l,k)}, \rho^{\text{in}}_{a(l,k)}, n_{a(l,k)}) \\
&= \eta_{\text{ad},a(l,k)} - \chi\left(\frac{q_{a(l,k)}}{\rho^{\text{in}}_{a(l,k)}}, n_{a(l,k)}; A^{\text{eff}}_{a(l,k)}\right),
\end{aligned}$$

where the volumetric flow rate $Q_{a(l,k)}$ is expressed as $q_{a(l,k)}/\rho^{\text{in}}_{a(l,k)}$ and χ is the biquadratic polynomial from (2.46).

The curved lower and upper boundaries of the operating range are defined by the isolines of the speed limits, $n_{a(l,k)} \in [\underline{n}_{a(l,k)}, \overline{n}_{a(l,k)}]$. To the left, the operating range of the compressor machine is bounded by the *surgeline*,

$$0 \le c^{\text{surge}}_{a(l,k)}(q_{a(l,k)}, \rho^{\text{in}}_{a(l,k)}, H_{\text{ad},a(l,k)}) = \psi\left(\frac{q_{a(l,k)}}{\rho^{\text{in}}_{a(l,k)}}; \alpha^{\text{surge}}_{a(l,k)}\right) - H_{\text{ad},a(l,k)}.$$

To the right, the operating range is bounded by the *chokeline*,

$$0 \le c^{\text{choke}}_{a(l,k)}(q_{a(l,k)}, \rho^{\text{in}}_{a(l,k)}, H_{\text{ad},a(l,k)}) = H_{\text{ad},a(l,k)} - \psi\left(\frac{q_{a(l,k)}}{\rho^{\text{in}}_{a(l,k)}}; \alpha^{\text{choke}}_{a(l,k)}\right).$$

For the quadratic polynomial ψ see (2.45). In summary, the complete model of a turbo compressor reads

$$\begin{aligned}
0 &= c_{\mathscr{E},a(l,k)}(x^{\text{base}}_a, x_{a,l}, x_{a,l+1}, x_{a(l,k)}) \\
&= \begin{pmatrix}
c^{\text{base}}_{a(l,k)}(x^{\text{base}}_a, x_{a,l}, x_{a,l+1}, x^{\text{base}}_{a(l,k)}) \\
c^{\text{speed}}_{a(l,k)}(H_{\text{ad},a(l,k)}, q_{a(l,k)}, \rho^{\text{in}}_{a(l,k)}, n_{a(l,k)}) \\
c^{\text{eff}}_{a(l,k)}(\eta_{\text{ad},a(l,k)}, q_{a(l,k)}, \rho^{\text{in}}_{a(l,k)}, n_{a(l,k)})
\end{pmatrix}, \\
0 &\le c_{\mathscr{I},a(l,k)}(x_{a,l}, x_{a,l+1}, x_{a(l,k)}) = \begin{pmatrix}
c^{\text{surge}}_{a(l,k)}(q_{a(l,k)}, \rho^{\text{in}}_{a(l,k)}, H_{\text{ad},a(l,k)}) \\
c^{\text{choke}}_{a(l,k)}(q_{a(l,k)}, \rho^{\text{in}}_{a(l,k)}, H_{\text{ad},a(l,k)})
\end{pmatrix}.
\end{aligned}$$

The only additional variable besides $x^{\text{base}}_{a(l,k)}$ is the shaft speed $n_{a(l,k)}$,

$$x_{a(l,k)} = (x^{\text{base}}_{a(l,k)}, n_{a(l,k)}).$$

Piston compressor Piston compressors are designed to generate high compression ratios with moderate throughput. This type of compressor machines appears less frequently than turbo compressors; see again Section 2.3.5.1 for more details.

The characteristic diagram of a piston compressor is defined in the coordinates volumetric flow Q and shaft torque M; it has a simple box shape as illustrated in Figure 2.4(b). The volumetric flow through a piston compressor depends on the operating volume $V_{\mathrm{o},a(l,k)}$ (the volume of gas that is compressed during one cycle) and the speed of the crankshaft that drives the machine:

$$0 = c^{\mathrm{vol}}_{a(l,k)}(q_{a(l,k)}, \rho^{\mathrm{in}}_{a(l,k)}, n_{a(l,k)}) = \frac{q_{a(l,k)}}{\rho^{\mathrm{in}}_{a(l,k)}} - V_{\mathrm{o},a(l,k)} n_{a(l,k)}.$$

Since the shaft speed is bounded by $n_{a(l,k)} \in [\underline{n}_{a(l,k)}, \overline{n}_{a(l,k)}]$, one obtains corresponding limits of the volumetric flow as left and right boundaries of the operating range. The shaft torque $M_{a(l,k)}$ is given by the constraint

$$0 = c^{\mathrm{torque}}_{a(l,k)}(\rho^{\mathrm{in}}_{a(l,k)}, M_{a(l,k)}, H_{\mathrm{ad},a(l,k)}) = M_{a(l,k)} - \frac{V_{\mathrm{o},a(l,k)} H_{\mathrm{ad},a(l,k)}}{2\pi\eta_{\mathrm{ad},a(l,k)}} \rho^{\mathrm{in}}_{a(l,k)},$$

where $\rho^{\mathrm{in}}_{a(l,k)}$ denotes the gas density at the compressor inlet. For piston compressors, the adiabatic efficiency $\eta_{\mathrm{ad},a(l,k)}$ is a constant parameter. Depending on the specific machine and the available technical data, the compression ability is limited in one of the following ways:

$$0 \le c^{\mathrm{limit}}(p_{a,l}, p_{a,l+1}, M_{a(l,k)}) = \begin{cases} \overline{\varepsilon} - p_{a,l+1}/p_{a,l}, \\ p_{a,l} - p_{a,l+1} + \overline{\Delta p}, \\ \overline{M}_{a(l,k)} - M_{a(l,k)}. \end{cases}$$

Here $\overline{\varepsilon}$ denotes an upper limit on the compression ratio, $\overline{\Delta p}$ an upper limit on the pressure increase, and $\overline{M}_{a(l,k)}$ an upper torque bound.

In summary, a piston compressor is modeled by the constraints

$$0 = c_{\mathcal{E},a(l,k)}(x^{\mathrm{base}}_a, x_{a,l}, x_{a,l+1}, x_{a(l,k)}) = \begin{pmatrix} c^{\mathrm{base}}_{a(l,k)}(x^{\mathrm{base}}_a, x_{a,l}, x_{a,l+1}, x^{\mathrm{base}}_{a(l,k)}) \\ c^{\mathrm{torque}}_{a(l,k)}(\rho^{\mathrm{in}}_{a(l,k)}, M_{a(l,k)}, H_{\mathrm{ad},a(l,k)}) \\ c^{\mathrm{vol}}_{a(l,k)}(q_{a(l,k)}, \rho^{\mathrm{in}}_{a(l,k)}, n_{a(l,k)}) \end{pmatrix},$$

$$0 \le c_{\mathcal{I},a(l,k)}(x_{a,l}, x_{a,l+1}, x_{a(l,k)}) = c^{\mathrm{limit}}(p_{a,l}, p_{a,l+1}, M_{a(l,k)}),$$

and the variables

$$x_{a(l,k)} = (x^{\mathrm{base}}_{a(l,k)}, M_{a(l,k)}, n_{a(l,k)}).$$

10.1.10.3 ▪ Compressor drives

Drives deliver the power required by compressor machines. The drive d associated with a compressor machine $a(l,k)$ is given by a mapping σ from the set of compressors to the set of drives, i.e., we have $d = \sigma(a(l,k))$ if drive d is associated to compressor $a(l,k)$. While every compressor is attached to a unique drive, some compressors may share a drive, i.e., a single drive may power several compressor machines. To simplify the exposition in this section, we describe in detail only the case where every drive powers just one compressor machine. The resulting model is easily extended to the general case.

Drives are categorized into three different types based on the energy source and the design principle: *gas turbines*, *gas driven motors*, and *electric motors*.

Electrical motors use electrical power. They form the set of *electricity consuming drives* that we call $\mathbb{D}_{\text{el}}$ in the following.

In contrast, gas turbines and gas driven motors use gas from the network as their energy source. Specifically, they take their fuel gas from the inlet of the compressor group. These drives constitute the set of *gas consuming drives*, $\mathbb{D}_{\text{gas}}$. The fuel consumption q_d^{fuel} of a drive $d \in \mathbb{D}_{\text{gas}}$ is modeled by

$$0 = c_d^{\text{fuel}}(q_d^{\text{fuel}}, b_d, m_a, H_{\text{c},a}) = q_d^{\text{fuel}} - \frac{b_d\, m_a}{H_{\text{u},a}};$$

see Section 2.3.5.4 for a more detailed description. Here, $H_{\text{u},a} = c\, H_{\text{c},a}$ denotes the lower calorific value, which differs from the (upper) calorific value $H_{\text{c},a}$ by a constant factor c (see Cerbe (2008)). In practice, the fuel gas is taken from the network. To consider this in a model with fixed and balanced supply and demand, the required fuel gas needs to be known to adjust supply or demand accordingly. Since the required fuel gas is not known a priori, its extraction from the network is not modeled. See Chapter 5 for more details.

The maximal power $\overline{P}_d$ that a drive d can deliver is the upper bound on the power $P_{a(l,k)}$ consumed by the connected compressor machine:

$$0 \le c_{\mathcal{I},d}(P_{a(l,k)}, \overline{P}_d) = \overline{P}_d - P_{a(l,k)}, \quad d = \sigma(a(l,k)). \tag{10.43}$$

If the drive powers several machines, $\overline{P}_d$ is the upper bound on the sum of the required compressor powers. The value $\overline{P}_d$ depends on the drive speed, which equals the speed of the connected compressor, $n_{a(l,k)}$, since compressors are directly mounted on the drive shaft. If several machines are connected, their speeds are therefore identical. In addition to (10.43), every type of drive requires for its model a specific subset of the drive variables, $x_d = (q_d^{\text{fuel}}, P_{a(l,k)}, \overline{P}_d, b_d)$, and a specific subset of the equations, see Section 2.3.5.4,

$$\begin{aligned}
0 &= c_d^{\text{spec-ener}}(b_d, P_{a(l,k)}) = b_d - \psi(P_{a(l,k)}; \alpha_d^{\text{energy}}),\\
0 &= c_d^{\text{biquad-power}}(\overline{P}_d, n_{a(l,k)}) = \overline{P}_d - \chi(n_{a(l,k)}, T_{\text{amb},a}; A_d^{\text{max-power}}),\\
0 &= c_d^{\text{quad-power}}(\overline{P}_d, n_{a(l,k)}) = \overline{P}_d - \psi(n_{a(l,k)}; \alpha_d^{\text{max-power}}).
\end{aligned}$$

Here, $\alpha_{b_d}, \alpha_{P,d}$, and $A_{P,d}$ are the corresponding coefficient vectors or coefficient matrix of the polynomials; see Section 2.3.5.4.

Gas turbines Gas turbines are modeled by the specific energy consumption rate b_d, which depends on the power consumed by the compressor, $P_{a(l,k)}$, and a relation between the power limit $\overline{P}_d$, the compressor speed $n_{a(l,k)}$, and the constant ambient temperature $T_{\text{amb},a}$. In terms of the above constraints the model reads

$$0 = c_{\mathcal{E},d}(x_{a(l,k)}, x_d) = \begin{pmatrix} c_d^{\text{fuel}}(q_d^{\text{fuel}}, b_d, m_a, H_{\text{c},a}) \\ c_d^{\text{spec-ener}}(b_d, P_{a(l,k)}) \\ c_d^{\text{biquad-power}}(\overline{P}_d, n_{a(l,k)}) \end{pmatrix}. \tag{10.44}$$

Gas driven motors Gas driven motors behave like gas turbines, except that the maximal power does not depend on the ambient temperature:

$$0 = c_{\mathcal{E},d}(x_{a(l,k)}, x_d) = \begin{pmatrix} c^{\text{fuel}}(q_d^{\text{fuel}}, b_d, m_a, H_{\text{c},a}) \\ c_d^{\text{spec-ener}}(b_d, P_{a(l,k)}) \\ c_d^{\text{quad-power}}(\overline{P}_d, n_{a(l,k)}) \end{pmatrix}.$$

Note that the difference to (10.44) is the usage of $c^{\text{quad-power}}$ instead of $c^{\text{biquad-power}}$.

Electric motors These drives consume electric power rather than fuel gas. Depending on the specific design, the ambient temperature may or may not have an influence on the power limit. An electric motor d is thus modeled by one of the following constraints:

$$0 = c_{\mathcal{E},d}(x_{a(l,k)}, x_d) = \begin{pmatrix} c_d^{\text{spec-ener}}(b_d, P_{a(l,k)}) \\ c_d^{\text{quad-power}}(\overline{P}_d, n_{a(l,k)}) \end{pmatrix}$$

or

$$0 = c_{\mathcal{E},d}(x_{a(l,k)}, x_d) = \begin{pmatrix} c_d^{\text{spec-ener}}(b_d, P_{a(l,k)}) \\ c_d^{\text{biquad-power}}(\overline{P}_d, n_{a(l,k)}) \end{pmatrix}.$$

10.1.10.4 ▪ Complete compressor group model

A generic model of an active compressor group is highly complex even though the active configuration is determined by the candidate solution of a decision approach. The model needs to incorporate several compression stages with their respective compressor machines and drives as well as the inlet and outlet resistors and the gas cooler. The constraints representing a compression stage $l = 1, \dots, s$ can be summarized as

$$\begin{aligned} 0 &= c_{\mathcal{E},a,(l,l+1)}(x_{a,l}, x_{a,l+1}, x_a^{\text{base}}, x_{a,(l,l+1)}) \\ &= \begin{pmatrix} c^{\text{flow-dist}}(q_a, (q_{a(l,k)})_{k=1}^{m_l}) \\ c^{\text{mix-temp}}((q_{a(l,k)})_{k=1}^{m_l}, T_{a,l+1}, (T_{a(l,k)}^{\text{out}})_{k=1}^{m_l}) \\ c_{\mathcal{E},a(l,k)}(x_a^{\text{base}}, x_{a,l}, x_{a,l+1}, x_{a(l,k)})_{k=1}^{m_l} \\ c_{\mathcal{E},\sigma(a(l,k))}(x_{a(l,k)}, x_{\sigma(a(l,k))})_{k=1}^{m_l} \end{pmatrix}, \\ 0 &\le c_{\mathcal{I},a,(l,l+1)}(x_{a,l}, x_{a,l+1}, x_{a,(l,l+1)}) \\ &= \begin{pmatrix} c_{\mathcal{I},a(l,k)}(x_{a,l}, x_{a,l+1}, x_{a(l,k)}) \\ c_{\mathcal{I},\sigma(a(l,k))}(P_{a(l,k)}, \overline{P}_{\sigma(a(l,k))}) \end{pmatrix}_{k=1}^{m_l}, \\ x_{a,(l,l+1)} &= ((x_{a(l,k)}, x_{\sigma(a(l,k))})_{k=1}^{m_l}). \end{aligned}$$

With these definitions, the complete model of a compressor group reads

$$0 = c_{\mathcal{E},a}(x_u, x_{a,v}, x_a) = \begin{pmatrix} c_{a,(0,1)}(x_{a,0}, x_{a,1}, x_a^{\text{base}}, x_{a,(0,1)}) \\ c_{\mathcal{E},a,(l,l+1)}(x_{a,l}, x_{a,l+1}, x_a^{\text{base}}, x_{a,(l,l+1)})_{l=1}^{s} \\ c_{a,(s+1,s+2)}(x_{a,s+1}, x_{a,s+2}, x_a^{\text{base}}, x_{a,(s+1,s+2)}) \\ c_{a,(s+2,s+3)}(p_{a,s+2}, p_v, T_{a,s+2}, T_{a:v}) \end{pmatrix}, \tag{10.45a}$$

$$0 \le c_{\mathcal{I},a}(x_a) = \left(c_{\mathcal{I},a,(l,l+1)}(x_{a,l}, x_{a,l+1}, x_{a,(l,l+1)})\right)_{l=1}^{s}, \tag{10.45b}$$

$$x_a = (x_a^{\text{base}}, (x_{a,l})_{l=1}^{s+2}, (x_{a,(l,l+1)})_{l=0}^{s+1}). \tag{10.45c}$$

10.1.11 ▪ Variable bounds

Almost all variables of the NLP model have lower or upper limits (or both) resulting from physical properties, technical restrictions, and legal requirements.

More restrictive bounds are typically given by technical limitations of the network elements. For instance, the maximal pressure reduction of a control valve station depends on the technical capabilities of the control valve, and the capabilities of compressor machines usually induce lower and upper bounds on the required power, specific change in adiabatic enthalpy, and volumetric flow. Of course, the values of technical bounds are determined by the specific design of every individual network device.

Finally, security prescriptions and legal requirements may induce even tighter limits. For instance, the gas temperature is typically kept between 273.15 K and 318.15 K to prevent critical processes like hydrate formation. Pipes are usually approved for a certain maximum pressure, which induces corresponding pressure bounds at the tail and head. Moreover, high-speed gas flow causes vibrations of the pipes. To reduce the resulting noise and to prevent damage of the pipes, the gas speed is bounded by some suitable value, depending on the pipe material.

Note that even wide physical bounds must be specified explicitly in certain cases to prevent the solution algorithms from generating invalid iterates. For instance, the compressibility factor cannot become smaller than zero in reality, but the AGA formula (10.4) and Papay's formula (10.5) can yield negative values of z for physically possible pressures and temperatures outside the ranges of validity of these formulas.

10.2 ▪ Objective functions

The detailed description of individual model components is now complete. We turn to the objective function before stating a complete NLP model. Depending on the specific planning task under consideration, various objectives can be of interest; we will present a few typical ones.

For the main problem considered in this book, the validation of nominations, any feasible solution is satisfactory, and a constant objective is formally sufficient. However, since we wish to obtain additional information if the NLP solver does not succeed in finding a feasible solution, we actually use a relaxed problem formulation, where the objective consists of minimizing a suitable slack norm; see Section 10.3. Moreover, a zero objective does not lead to a well-posed formulation, so we would need some proper objective for regularization in any case. From an economic perspective, the most natural goal is to minimize the cost of network operation, which is dominated by the energy costs of gas consuming drives $\mathbb{D}_{\text{gas}}$ and electrically powered drives $\mathbb{D}_{\text{el}}$. Gas coolers and gas preheaters also consume a certain amount of fuel gas, but this can be neglected when compared to the energy consumption of compressors. The resulting objective reads

$$f^{\text{cost}}(q^{\text{fuel}}_{\mathbb{D}_{\text{gas}}}, P_{\mathbb{D}_{\text{el}}}) = \sum_{d \in \mathbb{D}_{\text{gas}}} \omega_d q_d^{\text{fuel}} + \sum_{d \in \mathbb{D}_{\text{el}}} \omega_d P_d,$$

where q_d^{fuel} and P_d denote the mass flow and power consumed by drive d, and ω_d is a cost coefficient.

If electric power is available in abundance and hence cheap, one might also be interested in minimizing only the consumption of fuel gas,

$$f^{\text{fuel}}(q^{\text{fuel}}_{\mathbb{D}_{\text{gas}}}) = \sum_{d \in \mathbb{D}_{\text{gas}}} q_d^{\text{fuel}}.$$

A more ecological goal consists of minimizing the power consumption of compressors rather than the monetary cost of this power,

$$f^{\text{power}}(P_{A_{\text{cg}}}) = \sum_{a \in A_{\text{cg}}} \sum_{l=1}^{s_a} \sum_{k=1}^{m_l} P_{a(l,k)}.$$

10.3 ▪ Relaxations

The component models presented in the preceding sections satisfy the standard smoothness requirements stated at the beginning of this chapter. Hence standard NLP solvers can be applied, and the models are well suited to validate candidate solutions of the decision approaches. If this yields a feasible solution, the given solution candidate has been verified to be a valid approximation and has been adjusted to a more detailed model of gas physics and technical devices. Unfortunately, the opposite outcome does not provide much decisive information, since standard NLP solvers are *local* optimizers: if the problem is infeasible, they do not offer any hints to possible reasons, and they may fail to find feasible solutions even if they exist. On the other hand, the problem is much too hard to apply *global* solvers; otherwise we would not need the separate stages of decision approach and NLP validation in the first place.

To gain additional information in the case of unsuccessful NLP runs, we introduce slack variables σ^+ and σ^- and introduce relaxed versions of general NLP models like (10.1) instead:

$$\begin{aligned} \min_{x,\sigma^+,\sigma^-} \quad & f^{\text{relax}}(x,\sigma^+,\sigma^-) & & \\ \text{s.t.} \quad & c_i(x) + \sigma_i^+ - \sigma_i^- = 0, & & i \in \mathscr{E}, \\ & c_j(x) + \sigma_j^+ \geq 0, & & j \in \mathscr{I}, \\ & \sigma_i^+, \sigma_i^-, \sigma_j^+ \geq 0, & & i \in \mathscr{E},\ j \in \mathscr{I}, \\ & x \in [\underline{x}, \overline{x}]. & & \end{aligned} \tag{10.46}$$

The new objective function f^{relax} will be defined as a suitable norm of the slack variables, so that we minimize some measure of infeasibility. In fact, the relaxed NLP is feasible as long as $\underline{x} \leq \overline{x}$, and the x component of any optimal solution to (10.46) is a feasible point of the original problem (10.1) *if and only if* the objective value of (10.46) is zero, i.e., if all slack variables vanish. If this is not the case, the nonzero slack components give some indication which constraints are hard to satisfy in a heuristic sense.

The standard choice of f^{relax} is the ℓ_1-norm,

$$f^{\text{relax}}(x,\sigma^+,\sigma^-) = \left\|(\sigma^+,\sigma^-)\right\|_1 = \sum_{i \in \mathscr{E} \cup \mathscr{I}} \sigma_i^+ + \sum_{i \in \mathscr{E}} \sigma^-.$$

If the objective value is positive, this choice of f^{relax} tends to produce only a small number of nonzero slack variables, which may indicate what components or areas of the gas network "cause" the infeasibility. This kind of information proves to be quite useful to practitioners (see Chapter 11, too).

A second natural choice of the objective function is the ℓ_∞-norm, which is obtained by minimizing an upper bound $\overline{\sigma}$ on all slack variables,

$$f^{\text{relax}}(x,\sigma^+,\sigma^-,\overline{\sigma}) = \overline{\sigma}, \quad \sigma_i^+, \sigma_i^-, \sigma_j^+ \leq \overline{\sigma}, \quad i \in \mathscr{E},\ j \in \mathscr{I}.$$

This objective, however, does not offer any insight into possible reasons for infeasibility, since a nonzero objective value tends to produce a large number of nonzero slack values. For a discussion of the different norms see Section 11.6. The relaxation idea can be applied to our gas network model in several ways. While feasibility of (10.46) is only guaranteed when all constraints are relaxed, it is often sufficient to apply the relaxation to a suitable subset. For example, a restriction to special types of network elements, like compressor groups or pipes, can increase the chance to obtain useful information from the nonzero slack variables. Similarly, a relaxation of the flow balance equations (10.10) can be useful to detect obstructive, possibly implicit, flow restrictions.

10.4 ▪ A concrete validation model

In this section, we fix a single instantiation of the family of NLP models that have been presented in the preceding sections. This model is called ValNLP in the following and is used for the computational experiments in Chapter 12.

For choosing the concrete model variants, often a compromise between physical and technical accuracy on the one hand and solvability of the model on the other hand is necessary. Most of the model choices correspond to the component models of compressors and pipes. For pipes, we choose a model that is similar to the pipe models of the decision approaches, i.e., we use

- ▷ the quadratic approximation (10.21) of the pressure loss along a pipe,
- ▷ the mean pressure approximation, see (10.24),
- ▷ the smooth friction approximation (10.18), and
- ▷ the AGA formula (2.5).

For compressors and drives, we use a model incorporating

- ▷ the complete machine models with characteristic diagrams of turbo and piston compressors,
- ▷ the complete drive model, see Section 10.1.10.3, and
- ▷ a constant isentropic exponent, see (10.40).

We also choose to not include any mixing constraints for the gas parameters. In particular, this concrete model does not handle mixing of calorific values, but is applied to flow nominations derived from power nominations assuming an average calorific value as described in Section 5.3.3.

To be precise, ValNLP is given by

$$\begin{aligned}
\min_{x,\sigma^+,\sigma^-} \quad & f^{\text{relax}}(x,\sigma^+,\sigma^-) && (10.47)\\
\text{s.t.} \quad & (10.10) \quad \text{for all } u \in V,\\
& (10.25), (10.26) \quad \text{for all } a \in A_{\text{pi}},\\
& (10.28) \quad \text{for all } a \in A_{\text{lin-rs}},\\
& (10.29) \quad \text{for all } a \in A_{\text{nl-rs}},\\
& (10.30) \quad \text{for all } a \in A_{\text{va}}\,(a \text{ open}), a \in A_{\text{sc}}, a \in A_{\text{cg}} \cup A_{\text{cv}}\,(a \text{ in bypass}),\\
& (10.31) \quad \text{for all } a \in A_{\text{va}}\,(a \text{ closed}), a \in A_{\text{cg}} \cup A_{\text{cv}}\,(a \text{ closed}),\\
& (10.34) \quad \text{for all } a \in A_{\text{cv}}\,(a \text{ active}),\\
& (10.45) \quad \text{for all } a \in A_{\text{cg}}\,(a \text{ active}),\\
& x \in [\underline{x}, \overline{x}].
\end{aligned}$$

The variable vector x consists of all variables required by the constraints. In addition, all nonlinear constraints of (10.47) are relaxed, leading to according slack variable vectors σ^+ and σ^-. Finally, we remark that we use the ℓ_1-norm as the measure of infeasibility in the objective function $f^{\text{relax}}(x, \sigma^+, \sigma^-)$.